International Journal of Solids and Structures 47 (2010) 3166–3185

Contents lists available at ScienceDirect

International Journal of Solids and Structures

journal homepage: www.elsevier.com/locate/ijsolstr

A generalized anisotropic failure criterion for geomaterials

Zhiwei Gao [a], Jidong Zhao [a,*], Yangping Yao [b]

[a] Dept of Civil and Environmental Engineering, the Hong Kong University of Science and Technology, Clearwater Bay, Kowloon, Hong Kong SAR, China
[b] Dept of Civil Engineering, Beihang University, Beijing, China

ARTICLE INFO

Article history:
Received 6 May 2010
Received in revised form 16 July 2010
Available online 3 August 2010

Keywords:
Anisotropy
Failure criterion
Geomaterials
Shear strength
Triaxial tests
Torsional shear

ABSTRACT

Experimental evidence shows that the strength of geomaterials, such as soils and rocks, is significantly influenced by inherent anisotropy and other factors such as shear banding and the intermediate principal stress, which cannot be properly described by an isotropic failure criterion. This paper presents a generalized failure criterion for geomaterials with cross-anisotropy. To account for the influence of cross-anisotropy, we introduce an anisotropic variable in terms of the invariants and joint invariants of the stress tensor and the fabric tensor into the frictional coefficient of the failure criterion. The anisotropic failure criterion is formulated in both the deviatoric plane and the meridian plane which collectively offer a general three-dimensional description of strength anisotropy. All the parameters introduced in the criterion can be conveniently determined by conventional laboratory tests. We demonstrate that the new criterion is general and robust in describing the variation of strength with loading direction for a wide range of materials. The failure criterion has been applied to the prediction of strength for several clays, sands and rocks reported in the literature. The predictions compare favorably with available experimental data. Further discussion is made on possible improvement of the new criterion to address other materials with complex strength characteristics, as well as its potential usefulness for constitutive modeling of anisotropic geomaterials.

1. Introduction

Inherent anisotropy is commonly observed in geomaterials such as soils and rocks. It is attributed to the depositional process and grain, void and/or crack characteristics of the soil or rock mass (Oda and Nakayama, 1989; Duveau et al., 1998; Mitchell and Soga, 2005). Frequently, the inherent anisotropy in a soil or rock takes the form of cross-anisotropy (or transverse-isotropy) characterized by one direction with distinctive anisotropy perpendicular to a bedding or lamination plane wherein it is largely isotropic (Kirkgard and Lade, 1993; Abelev and Lade, 2004; Niandou et al., 1997). This perpendicular direction, normally coincident with the direction of deposition, is referred to as the axis of anisotropy.

Inherent anisotropy has long been recognized to have a remarkable influence on the strength[1] of geomaterials which are important to a variety of geotechnical structures, such as footings, retaining walls and slopes (Casagrande and Carillo, 1944; Arthur and Menzies, 1972; Oda et al., 1978). Duncan and Seed (1966) were among the first who found the undrained strength of clay varies considerably with direction, and they attributed this phenomenon to the presence of preferred oriented fabric in clay. Experimental data on sensitive clay have also showed that the unconfined compression strength varies continuously with loading directions and the minimum strength observed is about 60% to 75% of the maximum (Yong and Silvestri, 1979). True triaxial tests on isotropically consolidated San Francisco Bay Mud by Kirkgard and Lade (1991, 1993) also demonstrated strong variation of strength with changing of relative orientation between the direction of deposition and that of the major principal stress. A more recent study by Nishimura et al. (2007) on natural London clay found a strong directional dependence of strength of this soil which is attributable to cross-anisotropy. Meanwhile, the influence of inherent anisotropy on soil strength is also evident in various experimental studies on sand, such as the triaxial compression tests (Oda, 1972), true triaxial tests (Yamada and Ishihara, 1979; Ochiai and Lade, 1983; Miura and Toki, 1984), the hollow cylinder tests (Hight et al., 1983; Tatsuoka et al., 1986a,b; Pradhan et al., 1988; Lade et al., 2008), plane strain tests (Tatsuoka et al., 1986a,b; Lam and Tatsuoka, 1988) and others (Guo, 2008). In investigating the bearing capacity of two model strip foundations built on the same sand, Oda et al. (1978) found that the difference in bearing capacity for the model with load perpendicular to the bedding plane and the other one with a parallel load to the bedding plane can reach as much as 34%. The attribution of cross-anisotropy to the sand strength in this case is indeed significant. In rocks, the influence of cross-anisotropy on shear strength is even more

* Corresponding author. Tel.: +852 2358 8418; fax: +852 2358 1534.
E-mail address: Jzhao@ust.hk (J. Zhao).

[1] The strength refers here to the peak failure stress attainable for ductile materials and the rupture stress for brittle materials.

0020-7683/$ - see front matter © 2010 Elsevier Ltd. All rights reserved.
doi:10.1016/j.ijsolstr.2010.07.016

Nomenclature

A	anisotropic variable
b	intermediate principal stress ratio
d	parameter characterizing the degree of strength anisotropy
d_{ij}	deviatoric fabric tensor
e	void ratio
F_{ij}	fabric tensor characterizing the initial microstructure anisotropy
I_1, I_2, I_3	invariants of the stress tensor
$\bar{I}_1, \bar{I}_2, \bar{I}_3$	invariants of the transformed stress tensor
M_f	parameter describing the frictional characteristics
n	parameter describing the hydrostatic pressure effect
p	mean stress
$\bar{p}$	transformed mean stress
p_r	reference pressure
q	deviatoric stress
q^*	deviatoric stress at failure in the triaxial compression shear mode
$\bar{q}^*$	transformed deviatoric stress at failure in the triaxial compression shear mode
q^*_M, q^*_S	deviatoric stress at failure in the triaxial compression shear mode for the extended Mises criterion and SMP criterion, respectively
s_{ij}	deviatoric stress tensor
α	parameter controlling the shape of the failure surface of Yao's isotropic failure criterion in the deviatoric plane
β	parameter characterizing the strength anisotropic effect
Δ	parameter characterizing the degree of inherent microstructure anisotropy
δ_{ij}	Kronecker delta
ζ	angle between the major principal stress direction and the axis of anisotropy in the hollow cylinder torsional shear tests
θ	angle between the current stress state and the vertical stress axes in the deviatoric plane (see Fig. 3)
ξ	angle between the vertical stress and axis of anisotropy in true triaxial tests
σ_0	triaxial tensile strength
$\sigma_1, \sigma_2, \sigma_3$	major, intermediate and minor principal stress respectively
$\bar{\sigma}_1, \bar{\sigma}_2, \bar{\sigma}_3$	transformed major, intermediate and minor principal stress, respectively
σ_c	confining pressure in triaxial compression tests
σ_{ij}	stress tensor
$\bar{\sigma}_{ij}$	transformed stress tensor
$\sigma_x, \sigma_y, \sigma_z$	stresses in the x, y and z directions respectively
$\sigma_r, \sigma_\theta, \sigma_{z\theta}$	radial, circumferential, and shear stress in the cylinder torsional shear tests, respectively
φ	friction angle
φ_0	reference friction angle
φ_c	friction angle in the triaxial compression shear mode
φ_e	friction angle in the triaxial extension shear mode

remarkable. Numerous triaxial compression tests on sedimentary rocks have supported the observation of variable rock strength with loading directions (e.g., Attewell and Sandford, 1974; Niandou et al., 1997; Duveau et al., 1998 and reference therein). It has been found that maximum strengths are achieved for the rock specimens when the major principal stress direction is orthogonal/parallel to the bedding/lamination plane, whilst minimum strengths are observed when the major principal stress direction and the bedding/lamination plane has an angle between 30° and 60°. The difference in the two extreme strengths in rocks is many times greater than that in the soils.

The dependency of strength on inherent anisotropy is hence an important property of both soils and rocks which needs to be carefully considered in evaluating the performance of geomaterials relevant to various geostructures. In particular, the failure criterion for a soil or a rock needs to take into account the influence of inherent anisotropy and loading directions, in addition to the mean stress and the magnitude of the intermediate principal stress. In the past, a number of isotropic criteria have been formulated to model the general yielding and failure of geomaterials (e.g., Argyris et al., 1974; Matsuoka and Nakai, 1974; Lade and Duncan, 1975; Lade, 1977; Ottosen, 1977; van Eekelen, 1980; Kim and Lade, 1984; Houlsby, 1986), as well as some more recent ones such as Liu and Carter (2003), Yao et al. (2004) and Mortara (2008). Most of these well received isotropic failure criteria, however, may find difficulties in the interpretation of yielding and failure for anisotropic soils. Indeed, Kirkgard and Lade (1993) have compared their experimental data on isotropically consolidated San Francisco Bay Mud against predictions by Lade (1977)'s isotropic failure criterion. They found Lade's isotropic criterion can fit reasonably well for the failure stress points of specimens with the angle θ (see Fig. 3) in the range from 0° to 90° in the deviatoric plane. An appreciable discrepancy, however, has been observed between Lade's failure surface and the failure data points for tests conducted with θ greater than 90° wherein Lade's failure criterion generally overestimates the strength of the specimen. In cases like this, anisotropic failure criteria would become necessary indeed. The development of better failure criteria for geomaterials has also partly been driven by the practical importance of proper characterization of strength anisotropy to geotechnical engineering, e.g., safe design of footing foundations on sand.

There have been a number of attempts in the past on developing anisotropic failure criteria for geomaterials. Abelev and Lade (2004), for instance, have developed a 3D failure criterion for cross-anisotropic soils based on Lade (1977)'s isotropic failure criterion. By rotating the axes of the isotropic failure surface around the origin of the principal stress space, they introduced three model parameters which can be determined against experimental data by least-squares method. This model, as suggested by its authors, however, is only applicable when the loading direction and the depositional direction of the soil coincide with each other and there is no significant rotation of principal stresses occurring. The criterion might therefore have limited use for the interpretation of experimental results from non-proportional loading paths, such as that in torsional shear tests where the principal stress directions are rotated relative to the bedding planes in pluviated sand. In overcoming these limitations, Lade (2007, 2008) proposed a 3D failure criterion for both rotating and non-rotating stress conditions. In his study, Lade (2007, 2008) combined his isotropic criterion (Lade, 1977) and a cross-anisotropic form of the anisotropic failure criterion developed by Pietruszczak and Mroz (2000), and introduced three model parameters in his new criterion. This criterion has shown great potential in capturing the failure behavior of soils under general 3D conditions with stress rotations. Mortara (2009) has employed a formulation combining the Lode dependence of the behavior in the deviatoric plane and that in the meridian plane and proposed an anisotropic criterion for geomaterials. His study, however, has been confined to the conventional triaxial tests and the stress tensor has been assumed to be coaxial with the fabric tensor. A total of nine model parameters used in Mortara (2009)'s model would make it a challenging work for their

calibration. Other relevant studies on anisotropic failure criterion include the work by Duveau et al. (1998), Pietruszczak and Mroz (2000, 2001), Pietruszczak et al. (2002), Guo and Stolle (2005), Lee and Pietruszczak (2008), Azami et al. (2009) and Schweiger et al. (2009). Note that some of the investigations have been devoted for anisotropic rocks weakened by cracks and factures. Evidently, the topic on strength anisotropy has been a current focus of research due to its engineering significance. Unlike its isotropic counterpart, a widely accepted anisotropic failure criterion that is easy to calibrate and use has yet to be established.

In this paper, we propose a new anisotropic failure criterion that is general and robust enough to be capable of addressing the failure behavior for a wide range of soils and rocks with cross-anisotropy. The study is based on a previous version of isotropic failure criterion proposed by Yao et al. (2004). Following an idea similar to that used in Dafalias et al. (2004), we define an anisotropic variable A, in terms of invariants and joint invariants of the stress tensor and the fabric tensor. The frictional parameter in the new failure criterion is assumed to be a function of this anisotropic variable A. The failure criterion proposed here is a combination of formulations in both the meridian plane and the deviatoric plane. As a result, the general three-dimensional stress conditions can be effectively handled. Comparison with experimental results on both clay and sand shows the new anisotropic failure criterion can capture the strength anisotropy in soils with satisfaction. Meanwhile, all the relevant model parameters in the criterion can be conveniently determined through conventional laboratory tests, such as triaxial tests and torsional shear tests. Detailed procedures on calibrating these parameters are elaborated. We also demonstrate that the proposed anisotropic failure criterion is versatile enough to capture some of the important features of strength anisotropy in rocks.

2. Generalized anisotropic failure criterion

The generalized anisotropic failure criterion for geomaterials to be presented here is based on an isotropic failure criterion previously developed by Yao et al. (2004) for frictional materials. A brief introduction of this isotropic criterion is helpful for the subsequent description of our anisotropic criterion.

2.1. Isotropic failure criterion for frictional materials (Yao et al., 2004)

The isotropic failure criterion developed by Yao et al. (2004) is a combination of formulations in both the deviatoric plane and the meridian plane. Experimental evidence shows that, at certain hydrostatic pressure, the failure curves of geomaterials in the *plane* typically lie between the extended Mises circle (Drucker and Prager, 1952) and the Matsuoka–Nakai (or so-called Spatial Mobilized Plane, SMP in brief) curve-sided triangle (Matsuoka and Nakai, 1974), denoted by the α-curve as shown in Fig. 1. In this plane, Point A denotes a stress state at which the material fails. To characterize the α-curve, the following expression is employed for the corresponding deviatoric stress q^* in the triaxial compression shear mode

$$q^* = \alpha q_M^* + (1-\alpha) q_S^* \tag{1}$$

where q_M^* and q_S^* are, respectively, the corresponding deviatoric stress at the triaxial compression shear mode for the extended Mises criterion and SMP criterion passing through the same stress point A, which can be determined by:

$$q_M^* = \sqrt{I_1^2 - 3I_2} \tag{2}$$

$$q_S^* = \frac{2I_1}{3\sqrt{(I_1 I_2 - I_3)/(I_1 I_2 - 9I_3)} - 1} \tag{3}$$

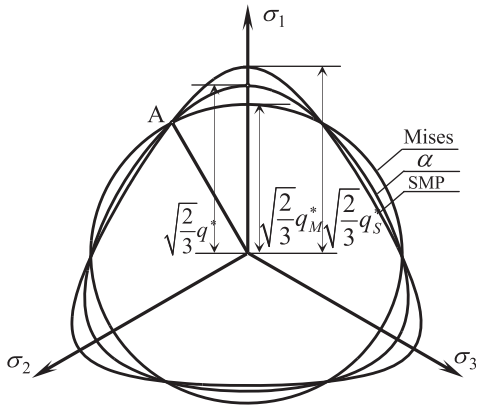

Fig. 1. Failure surface of the isotropic failure criterion in the deviatoric plane (Yao et al., 2004).

where $I_1(=\sigma_1+\sigma_2+\sigma_3)$, $I_2(=\sigma_1\sigma_2+\sigma_2\sigma_3+\sigma_3\sigma_1)$ and $I_3(=\sigma_1\sigma_2\sigma_3)$ are the invariants of the stress tensor σ_{ij}, with σ_1, σ_2 and σ_3 being the major, intermediate and minor principal stresses respectively; α is a material constant. It is readily verifiable that, if $\alpha = 1$, the α-curve coincides with the extended Mises criterion and presents as a circle in the deviatoric plane; and if $\alpha = 0$, it recovers the SMP curve-sided triangular shape in the deviatoric plane; if $0 < \alpha < 1$, it lies in between the extended Mises and SMP failure curves in this plane. The α-curve is indeed a generalization of both the extended Mises criterion and the SMP failure criterion in the deviatoric plane. Note that Mortara (2008, 2009) has proposed a general expression to generalize both SMP and Lade and Duncan criteria.

In the *meridian plane*, the following expression is adopted for the deviatoric stress at failure:

$$q^* = M_f \left(\frac{p+\sigma_0}{p_r}\right)^n p_r \tag{4}$$

where M_f pertains to the frictional characteristics of the material and represents the slope of the projected line in $\bar{p} - \bar{q}^*$ plane (as will be shown in Fig. 2). Its value generally varies from 0 to 3. σ_0 denotes the triaxial tensile strength of the material, which reflects the effect of cohesion. p is the mean stress and p_r is a reference pressure. The exponent n is used to address the effect of hydrostatic pressure on the failure of a material, and is a parameter controlling the curvature of the curve in the meridian plane. It is always preferable to have a linearized form of the relation in Eq. (4) which can be then used in conjunction with the failure function in the deviatoric plane.

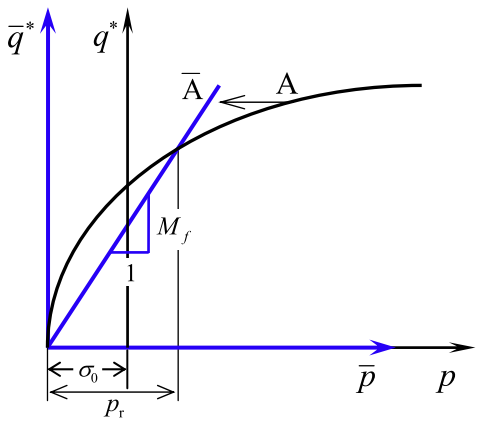

Fig. 2. Failure curve of the isotropic failure criterion in the meridian plane and its linearization (Yao et al., 2004).

We see that Eq. (4) is a monotonic function of p. As such, we can perform the following coordinate transformation for the linearization (as shown in Fig. 2)

$$\bar{q}^* = q^* \tag{5a}$$
$$\bar{q}^* = M_f \bar{p} \tag{5b}$$

It is readily found from Eqs. (4) and (5) that

$$\bar{p} = \frac{q^*}{M_f} = \left(\frac{p+\sigma_0}{p_r}\right)^n p_r \tag{6}$$

The following transformed stress tensor can then be defined to construct the failure criterion for a material in the general 3D stress space

$$\bar{\sigma}_{ij} = \sigma_{ij} + (\bar{p} - p)\delta_{ij} = \sigma_{ij} + \left[p_r\left(\frac{p+\sigma_0}{p_r}\right)^n - p\right]\delta_{ij} \tag{7}$$

where δ_{ij} is the Kronecker delta. By substituting q^* in Eq. (1) with $\bar{q}^*$ and using the above relations, the following failure criterion has been developed by Yao et al. (2004)

$$\alpha\sqrt{\bar{I}_1^2 - 3\bar{I}_2} + (1-\alpha)\frac{2\bar{I}_1}{3\sqrt{(\bar{I}_1\bar{I}_2 - \bar{I}_3)/(\bar{I}_1\bar{I}_2 - 9\bar{I}_3)} - 1} = M_f\bar{p} \tag{8}$$

where, $\bar{I}_1$, $\bar{I}_2$ and $\bar{I}_3$ are the invariants of the stress tensor $\bar{\sigma}_{ij}$, according to the same definitions for I_1, I_2 and I_3. Detailed formulations and application of this isotropic failure criterion can be found in Yao et al. (2004). In the following subsection, we endeavor to generalize this criterion to the case of anisotropy to describe a wide range of geomaterials including clay, sand and rock.

2.2. Generalized anisotropic failure criterion

2.2.1. Fabric tensor

To develop an anisotropic failure criterion, a suitable variable is required to quantify the degree and orientation of inherent anisotropy in the material. The fabric tensor firstly proposed by Brewer (1964) has been a popular option in this regard. It has been used to describe, for example, the preferred soil particle orientation, void size and its orientation (Oda and Nakayama, 1989; Muhunthan and Chameau, 1997). Fabric tensor in form of a symmetric second-order tensor has been frequently used to describe the fabric in soils and rocks (Oda and Nakayama, 1989; Pietruszczak et al., 2002). Higher-order fabric tensors have also been suggested for the description of fabric based on various justifications (Oda, 1984; Pietruszczak and Mroz, 2001). As mentioned in the Introduction, most geomaterials are cross-anisotropic. As such, we follow the work by Oda and Nakayama (1989) in defining the inherent anisotropy in the material in this paper. Assume the principal axes of the material fabric is aligned with the reference coordinate (x_1,x_2,x_3), with the $x_2 - x_3$ plane being the isotropic plane, and x_1 directs to the axis of anisotropy. The following fabric tensor is adopted for the description of the cross-anisotropy

$$F_{ij} = \begin{bmatrix} F_1 & 0 & 0 \\ 0 & F_2 & 0 \\ 0 & 0 & F_3 \end{bmatrix} = \frac{1}{3+\Delta}\begin{bmatrix} 1-\Delta & 0 & 0 \\ 0 & 1+\Delta & 0 \\ 0 & 0 & 1+\Delta \end{bmatrix} \tag{9}$$

where Δ is a scalar that characterizes the magnitude of the cross-anisotropy. Its value ranges from zero when the material is absolutely isotropic, to unity when the degree of anisotropy is the maximum.

2.2.2. Anisotropic variable

According to the representation theorem developed by Wang (1970), a general expression for the failure criterion of an anisotropic geomaterial needs to be a function of the invariants and joint invariants of the stress tensor and the fabric tensor, e.g.:

$$\begin{aligned} f = f(\sigma_{ij}, F_{ij}) = f\big[&\mathrm{tr}(\sigma_{ij}), \mathrm{tr}(\sigma_{ik}\sigma_{kj}), \mathrm{tr}(\sigma_{ik}\sigma_{km}\sigma_{mj}), \mathrm{tr}(F_{ij}), \mathrm{tr}(F_{ik}F_{kj}), \\ &\mathrm{tr}(F_{ik}F_{km}F_{mj}), \mathrm{tr}(\sigma_{ik}F_{kj}), \mathrm{tr}(\sigma_{ik}\sigma_{km}F_{mj}), \mathrm{tr}(\sigma_{ik}F_{km}F_{mj}), \\ &\mathrm{tr}(\sigma_{ik}\sigma_{km}F_{mn}F_{nj})\big] = 0 \end{aligned} \tag{10}$$

To avoid excessive complication, we only consider some of the above invariants and joint invariants in our development. In particular, following the work by Dafalias et al. (2004), we choose the following variable A which presents a normalized form of the joint invariant of the deviatoric stress tensor and the deviatoric fabric tensor, to enter the yield criterion

$$A = \frac{\mathrm{tr}(s_{ik}d_{kj})}{\sqrt{s_{mn}s_{mn}}\sqrt{d_{pq}d_{pq}}} \tag{11}$$

where $s_{ij} = \sigma_{ij} - p\delta_{ij}$, $d_{ij} = F_{ij} - F_{kk}\delta_{ij}/3$, denoting the deviatoric stress tensor and deviatoric fabric tensor, respectively. The anisotropic variable A defined above can actually be conveniently used to characterize the loading direction with respect to the fabric orientation. In the case that the stress tensor and the fabric tensor are coaxial, the value of A is readily found to vary from -1 in the conventional triaxial compression shear mode to 1 in the conventional triaxial extension shear mode. In addition to the loading direction, experimental evidence also shows that the degree of anisotropy affects the properties of yielding and strength of geomaterials (Li and Dafalias, 2002; Yang et al., 2008). Additional parameters, such as the Δ used in Eq. (9), are required to develop a more realistic failure criterion. This issue will be addressed later.

It is desirable that the model parameters introduced in any failure criterion can be calibrated by routine testing means that are commonly available in the laboratory. For the present failure criterion, we will determine the parameters involved by such approaches as the true triaxial tests and hollow cylinder torsion shear tests. The conventional triaxial compression/extension tests will be used as complementary means. As for rocks, triaxial compression tests with different loading directions are commonly adopted for the purpose of calibration. To interpret true triaxial test results on soils with cross-anisotropy, we employ a Cartesian coordinate system as shown in Fig. 3. Note that similar coordinate system has been used by Ochiai and Lade (1983). Accordingly, the deviatoric plane can be divided into three unique sectors (I, II and III as shown in the figure).[2] The stress direction is assumed to be fixed with the reference coordinate (x,y,z). In true triaxial tests, it is common to set up the specimen with the axis of anisotropy being rotated by an angle of ξ with respect to *the vertical direction*, in either the $y-z$ plane or $x-z$ plane, to generate a non-coaxial condition between the stress tensor and the fabric tensor (Lam and Tatsuoka, 1988). Evidently, If $\xi = 0$, the fabric tensor becomes coaxial with the stress tensor, which is the case that was treated by Ochiai and Lade (1983). Assuming that the axis of anisotropy is rotated in the $y-z$ plane and using the intermediate principal stress ratio defined by Habib (1953) (see also, Bishop, 1971) $b = (\sigma_2 - \sigma_3)/(\sigma_1 - \sigma_3)$, the anisotropic variable A in Eq. (11) can be expressed as follows in the three sectors as shown in Fig. 3:

(1) Sector I ($0^\circ \leqslant \theta \leqslant 60^\circ$)

$$A = \frac{(4b-5)\cos^2\xi + (4-5b)\sin^2\xi - (b+1)}{6\sqrt{b^2-b+1}} \tag{12}$$

(2) Sector II ($60^\circ \leqslant \theta \leqslant 120^\circ$)

[2] Note that the same definition and notations of the three sectors as in Fig. 3 will be followed in the rest of the paper if discussion is concerned with the deviatoric plane.

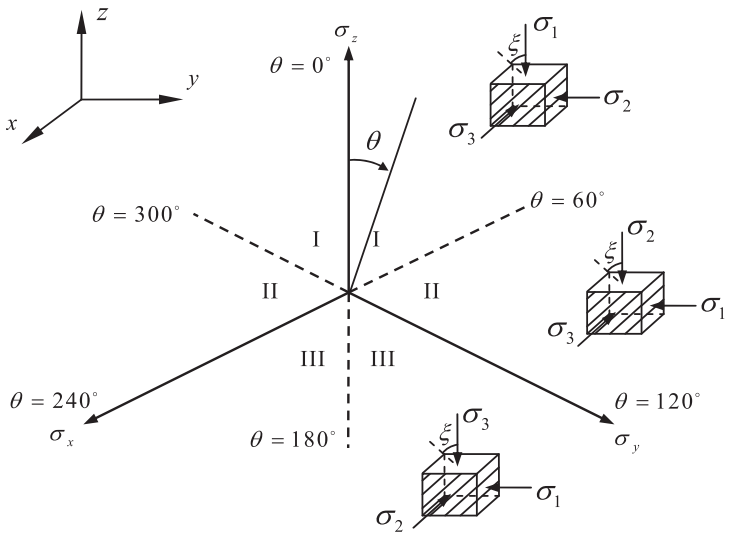

Fig. 3. Description of the true triaxial tests with initially inclined axis of anisotropy (c.f., Ochiai and Lade, 1983).

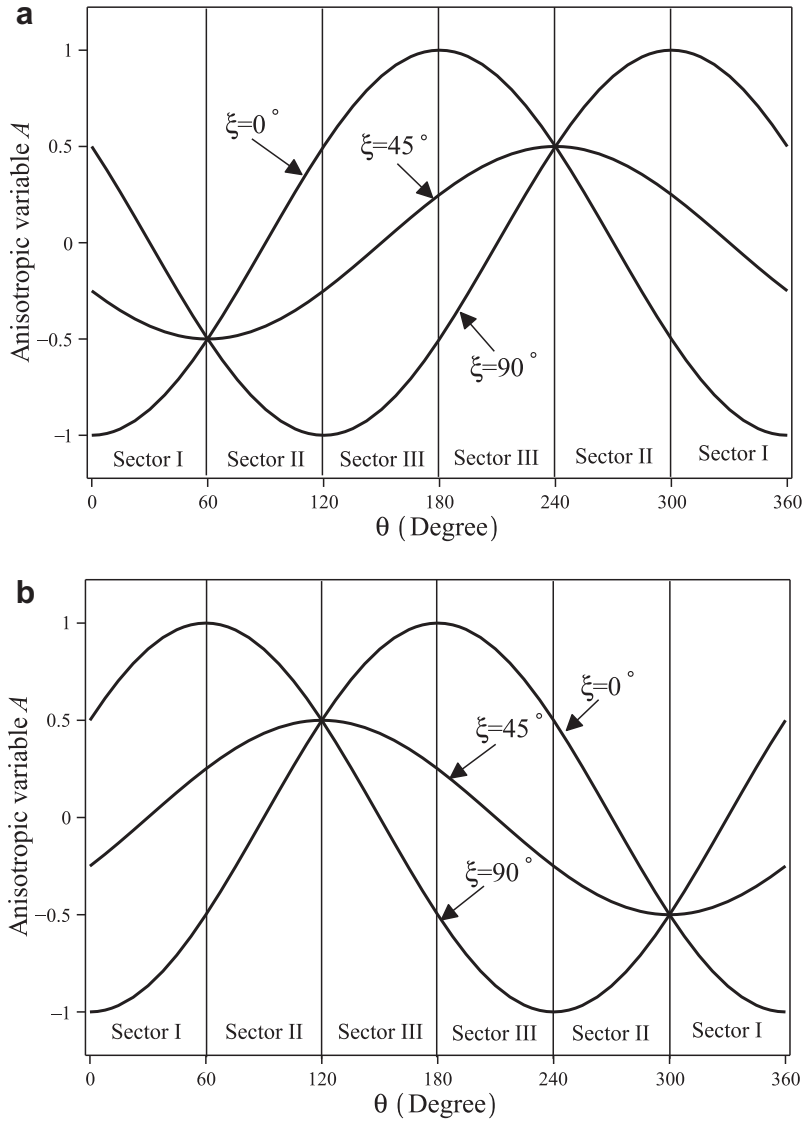

Fig. 4. Variation of A in true triaxial tests with θ when the axis of anisotropy is rotated by an angle of ξ with respect to the vertical direction in (a) the $y - z$ plane and (b) the $x - z$ plane.

$$A=\frac{(4-5b)\cos^2\xi+(4b-5)\sin^2\xi-(b+1)}{6\sqrt{b^2-b+1}} \tag{13}$$

(3) Sector III ($120^\circ \leqslant \theta \leqslant 180^\circ$)

$$A=\frac{(4+b)\cos^2\xi+(b-5)\sin^2\xi+2b-1}{6\sqrt{b^2-b+1}} \tag{14}$$

Similarly, when the axis of anisotropy is rotated in the $x-z$ plane, the expression for A can also be calculated. Fig. 4 shows the variation of A with θ in these two cases.

In the *hollow cylinder torsional shear tests*, the bedding plane is often oriented horizontally and the radial stress is the intermediate principal stress (Yoshimine et al., 1998). Shear stress is applied in the $z-\theta$ plane, and therefore, the major and minor principal stress direction is rotated by an angle of ζ relative to the axis of anisotropy as shown in Fig. 5. In this case, the expression of A can be expressed as follows

$$A=\frac{(b-5)\cos^2\zeta+(b+4)\sin^2\zeta+(2b-1)}{6\sqrt{b^2-b+1}} \tag{15}$$

The variation of A with ζ at different b values for the hollow cylinder torsion tests is shown in Fig. 6. Note that from Eq. (15), if $\zeta = 0$, $b = 0$, we have $A = -1$. This corresponds to the conventional triaxial compression shear mode; when $\zeta = 90^\circ$ and $b = 1$ such that $A = 1$, it corresponds to the conventional triaxial extension shear mode. Note that we use ζ to denote the angle between the *major principal stress direction* and the axis of anisotropy in a hollow cylinder specimen. Obviously ζ is generally not equivalent to ξ as the major principal stress direction does not always coincide with the vertical direction due to the complex stress state in a typical hollow cylinder shear test. By using the anisotropic variable A defined in Eqs. (12)–(15) for typical laboratory tests, we are now ready to generalize the isotropic failure criterion developed by Yao et al. (2004) to the anisotropic case.

2.2.3. Generalized anisotropic failure criterion

As indicated by Lade (2008), only those parameters that reflect the frictional characteristics of the material show a strong dependency with the loading direction. As such, we assume that, among all the parameters involved in the failure criterion, only the frictional coefficient, M_f, is dependent on the anisotropic variable A. Indeed, the experimental study by Imam et al. (2002) on the variation of M_f with the magnitude of the intermediate principal stress and loading direction on loose sand has supportive evidence on this. For the convenience of developing an anisotropic failure criterion, a reference state has been chosen by most past studies at which the anisotropic criterion provides the same prediction as the underlying isotropic criterion.[3] In developing their anisotropic failure criterion, Pietruszczak and Mroz (2001) have followed an approach to modify the parameters of isotropic failure criteria from their average values in three dimensions, and introduced a hypothetic isotropic state to represent an anisotropic state. Following this way, however, it is difficult to design appropriate laboratory tests for the calibration of such a hypothetic isotropic state. We hereby suggest that a shear mode that can be easily examined by conventional laboratory means be employed as a reference state. The conventional triaxial compression shear mode, for example, is an ideal option in this regard, as it facilitates the calibration of parameters relevant to the failure criterion in the meridian plane. This shear mode will thus be adopted in this paper as the reference shear mode.

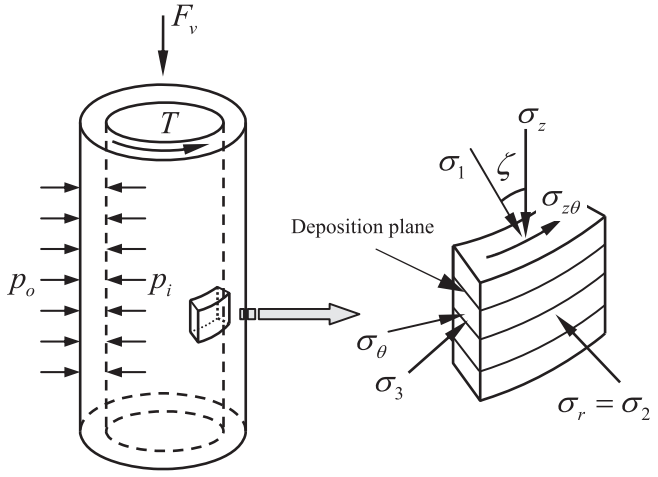

Fig. 5. Stress components on the hollow cylindrical specimen and the fabric orientation.

To sum up all the aspects mentioned above, we propose the following expression to describe the failure behavior of an anisotropic geomaterial

$$\alpha\sqrt{\bar{I}_1^2-3\bar{I}_2}+(1-\alpha)\frac{2\bar{I}_1}{3\sqrt{(\bar{I}_1\bar{I}_2-\bar{I}_3)/(\bar{I}_1\bar{I}_2-9\bar{I}_3)}-1} = M_f f(A)\bar{p} \tag{16}$$

where the function

$$f(A)=\exp\left\{d\left[(A+1)^2+\beta(A+1)\right]\right\} \tag{17}$$

is introduced as a modification of M_f in Eq. (8). As is seen in Eq. (17), in addition to the anisotropic variable A which reflects the influence of loading direction with respect to fabric, two more non-dimensional parameters, d and β are introduced. As will be demonstrated in the subsequent sections, d plays a role of measuring the degree of strength anisotropy for a material. When $d = 0$, we see that $f(A) \equiv 1$. In this case, the anisotropic failure criterion becomes identical to the underlying isotropic failure criterion in Eq. (8), irrespective of the loading direction. However, we note that d is not directly associated with Δ, as the degree of strength anisotropy is not necessarily equivalently reflected by the degree of fabric anisotropy relevant to the internal structures. The role of β in Eq. (17) is essentially to adjust the loading direction that leads to extreme values of $f(A)$. For instance, when $b = 0$, the expression of the failure criterion can be simplified as $\bar{q}/\bar{p} = M_f f(A)$. $f(A)$ can therefore be used as the only variable that controls the variation of the failure stress ratio $\bar{q}/\bar{p}$ with the loading direction. In the triaxial compression tests on rocks with different loading directions, as the angle ξ varies from 0° to 90°, the anisotropic variable A increases monotonically from -1 to *0.5* (refer to Eq. (12) with $b = 0$). Since d is typically chosen greater than zero, as will be shown in later sections, β essentially determines the loading direction in which the minimum value of $f(A)$, or equivalently the minimum failure stress ratio $\bar{q}/\bar{p}$, is attained. The overall effect of the function $f(A)$ is to change the shape of the underlying isotropic failure surface defined in Eq. (8) in the deviatoric plane. When $f(A) > 1$, the role it plays in Eq. (16) is to expand the failure surface with respect to the isotropic one, and to shrink it when $f(A) < 1$. In particular, when $A = -1$, $f(A) \equiv 1$. This corresponds to the reference conventional triaxial compression shear mode, and the anisotropic failure criterion is the same as the isotropic failure criterion shown in Eq. (8). Consequently, all the parameters controlling the failure curves in the meridian plane, M_f, σ_0 and n, can be directly determined from the conventional triaxial compression test data without considering the anisotropic effect.

[3] By saying so we implicitly assume that an anisotropic criterion is developed from some existing isotropic criteria, which is the case for most existing anisotropic criteria.

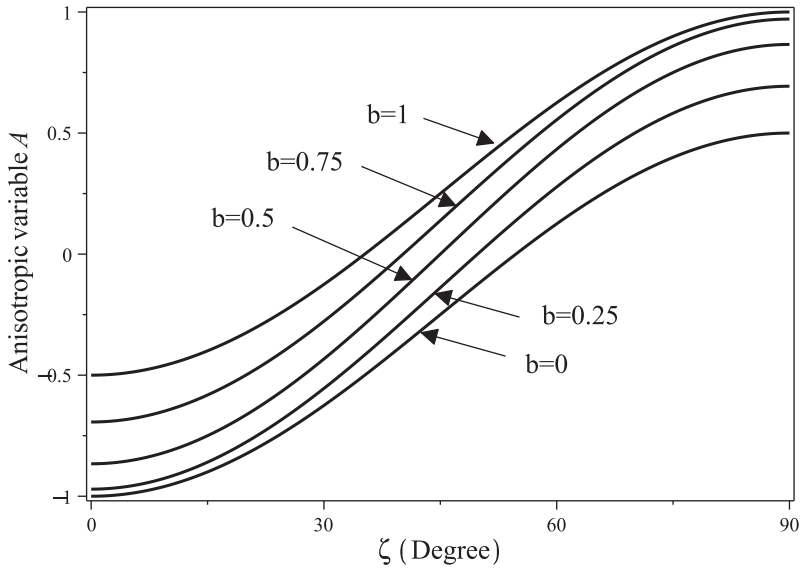

Fig. 6. Variation of A with ζ for different b values in the hollow cylinder torsional shear tests.

3. Parametric study

3.1. The effect of d and β on the failure curve in the deviatoric plane

The variations of the failure surface with β and d in the deviatoric plane are depicted in Figs. 7 and 8. Examinations have been carried out under the true triaxial test condition where the stress tensor and the fabric tensor are coaxial ($\xi = 0°$) as shown in Fig. 3. Two typical values of β, $\beta = -1.5$ and -2, have been used to examine the effect of d. As is shown in Fig. 7(a-1) and (a-2), when $\beta = -1.5$, the isotropic failure criterion and anisotropic failure criterion coincides at $\theta = 120°$ ($\theta = 0°$ is the reference state that automatically requires the two criteria to offer identical predictions). As d increases from 0 to 0.1, the failure curve shrinks inward

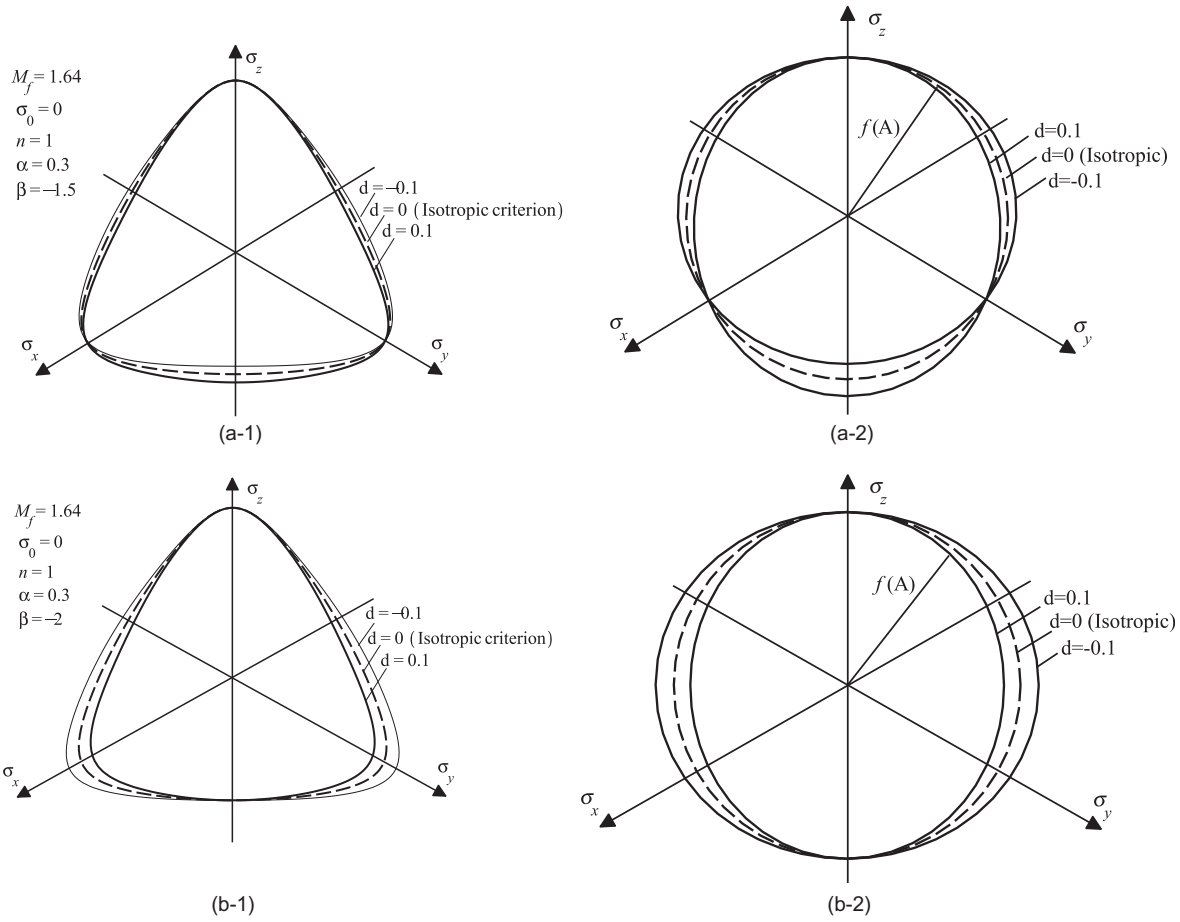

Fig. 7. Effect of d on the failure loci and $f(A)$ in the deviatoric plane with fixed β. (a-1) and (b-1) show the failure surface, and (a-2) and (b-2) demonstrate the shape of the function $f(A)$.

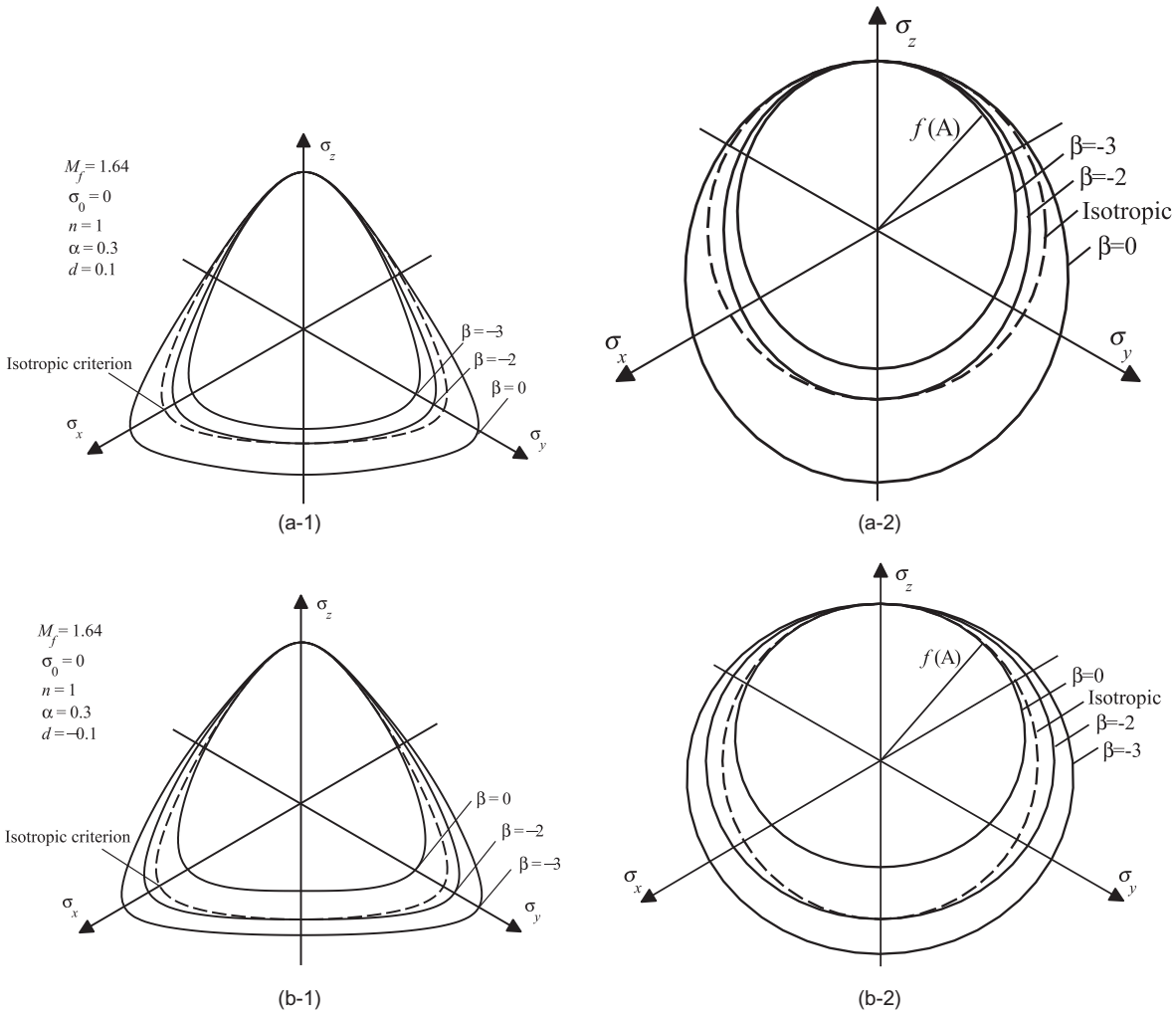

Fig. 8. Effect of β on the failure loci in the deviatoric plane with fixed d. (a-1) and (b-1) show the failure surfaces. (a-2) and (b-2) demonstrate the shape of the function $f(A)$.

in sectors I and II while expands outward in sector III. An opposite change is observed when d decreases from 0 to −0.1. In the case of $\beta = -2$ (Fig. 7(b-1) and (b-2)), the two failure criteria coincide at $\theta = 180°$ besides the reference state. Under this condition, the failure curve shrinks inwards as d increases. The effect of β on the failure loci with fixed d is illustrated in Fig. 8. The anisotropic failure criterion becomes identical to the isotropic one when $d = 0$. When $d > 0$, the anisotropic failure curve shrinks inwards as β decreases, and the opposite trend is obtained when $d < 0$.

3.2. Effect of the initial inclination of cross-anisotropy

Under the loading condition when the stress tensor and fabric tensor are non-coaxial as shown in Fig. 3 ($\xi > 0°$), the effect of the initial inclination of the axis of anisotropy on the failure curves in the deviatoric plane is illustrated in Fig. 9. The parameters are chosen with values as shown on the top corner of each figure. When $\xi = 0°$, the failure curve is symmetric about the σ_z axis. When the axis of anisotropy is rotated in the $y - z$ plane, the failure curve is symmetric about the σ_x axis at $\xi = 45°$, and about the σ_y axis at $\xi = 90°$. When the axis of anisotropy is rotated in the $x - z$ plane, the failure curve is symmetric about the σ_y axis at $\xi = 45°$, and about the σ_x axis at $\xi = 90°$. Since the failure curve is assumed to be a straight line in the meridian plane, it is not necessary to specify the value for the reference pressure.

4. Calibration of model parameters

There are some slight differences in the calibrating procedures for soils and for rocks, mainly due to the different routine experimental means available in practice for determining their strength. The procedures for the parameter calibration are hence presented in two separate subsections as follows, for soils and for rocks, respectively. In each subsection, we shall use one or more examples to demonstrate the process.

4.1. For soils

In triaxial tests where the stress and fabric tensors are coaxial as shown in Fig. 3, the general procedure for determining parameters in the proposed failure criterion is demonstrated as follows, followed by a particular case for the isotropically consolidated San Francisco reported in Kirkgard and Lade (1991, 1993).

4.1.1. Determination of σ_0, n and M_f

The parameters for the failure curve in the meridian plane will be determined first. It is reasonable to assume that soils can not sustain tensile stress if the interparticle bonds are not considered, as is the case for cohesionless soil. As such, we can assume $\sigma_0 = 0$ for convenience. It can be seen from Eq. (4) that n and M_f are dependent on the reference pressure p_r. Since α, d and β are calibrated based on the values chosen for n and M_f, they will depend

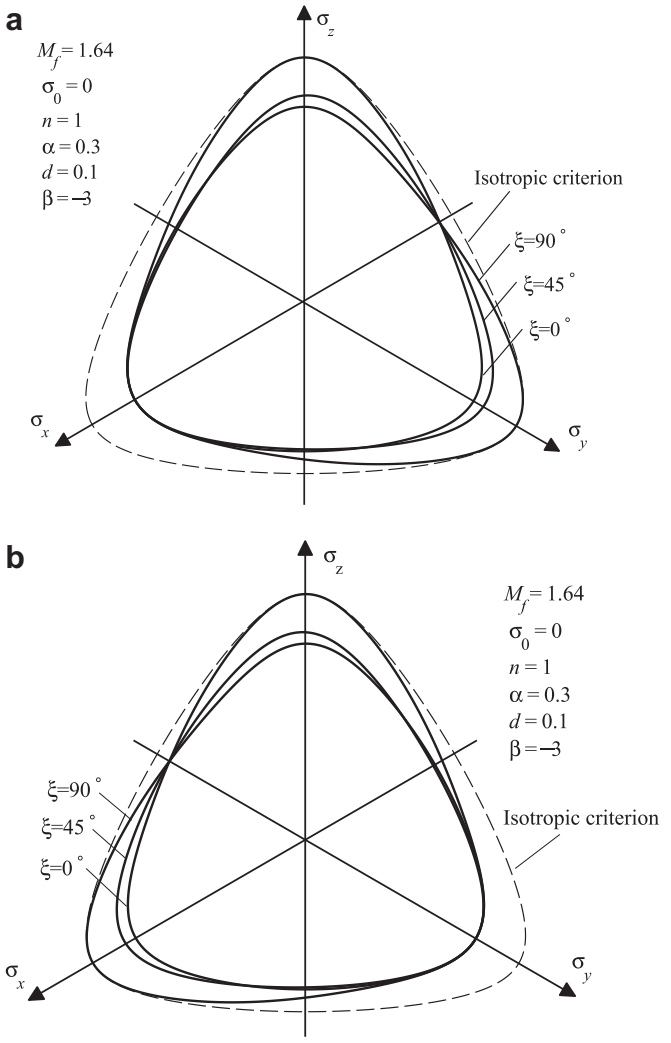

Fig. 9. Failure loci in the deviatoric plane with the axis of anisotropy rotated in (a) the $y-z$ plane and (b) the $x-z$ plane by an angle of ξ.

on p_r as well. It is recommended that p_r be chosen a value in the vicinity of the mean stress at failure. In order to determine n and M_f, the expression for the failure curve in the meridian plane, Eq. (4), is rearranged as follows

$$\ln\left(\frac{q^*}{p_r}\right) = \ln(M_f) + n\ln\left(\frac{p+\sigma_0}{p_r}\right) \tag{18}$$

which presents a straight line in the plane of $\ln\left(\frac{p+\sigma_0}{p_r}\right) \sim \ln\left(\frac{q^*}{p_r}\right)$ with a slope of n and intersection of $\ln(M_f)$ with respect to the vertical axis (as is shown in Fig. 10(a) for isotropically consolidated San Francisco Bay mud). By comparing against the experimental data points, M_f can then be back-calculated from the value of $\ln(M_f)$.

Note that from Eq. (4), if $n = 1$, the failure curve in the deviatoric plane is a straight line regardless of what value the reference pressure p_r is adopted. In this case, it is not necessary to specify the value of p_r explicitly. This actually applies to several cases of clays and sands to be treated in this paper.

4.1.2. Determination of α, d and β

The other parameters, α, d and β, can be determined based on the test results at $\theta = 60°$, 120° and 180°. The rationale for choosing the results in these shear modes is as follows.

(a) In triaxial tests on clays in all the three sectors as shown in Fig. 3, shear band is rarely observed, and therefore, most test results represent the behavior of a continuum soil body (Kirkgard and Lade, 1993; Lade and Kirkgard, 2000). However, in the tests on sand with midrange b values (Sector I: $0.3 < b < 0.9$; Sector II: $0.2 < b < 0.9$; Sector III: $0.2 < b < 0.8$), shear banding has been frequently observed in the hardening regime. The strength obtained in this range is not particularly reliable (Abelev and Lade, 2004). Nevertheless, as indicated by Abelev and Lade (2004), a smooth peak failure for sand, which corresponds to a homogeneous behavior, is always attainable in these three shear modes when $\theta = 60°$, 120° and 180°. Choosing the three shear modes for the calibration of relevant parameters is thus appropriate for both clay and sand.

(b) At these three shear modes, since b is either *0* or 1, the anisotropic failure criterion can be simplified to form certain linear equations of these parameters, which is helpful for the calibration as well.

As mentioned by Abelev and Lade (2004), the anisotropic effect is not significant in Sector I but relatively more pronounced in Sectors II and III for most soils. The test data in Section I can therefore be used to determine the parameters for the underlying isotropic criterion. The test results obtained at the shear mode of $\theta = 60°$ is chosen to determine α. In this shear mode, $\bar{\sigma}_1 = \bar{\sigma}_2 > \bar{\sigma}_3$ and $A = -0.5$, Eqs. (16) and (17) can be simplified as

$$\alpha(\bar{\sigma}_1 - \bar{\sigma}_3) + (1-\alpha)(\bar{\sigma}_1 - \bar{\sigma}_3)\frac{2\bar{\sigma}_1 + \bar{\sigma}_3}{\bar{\sigma}_1 + 2\bar{\sigma}_3} = M_f\bar{p}\exp\left[d(0.25 + 0.5\beta)\right] \approx M_f\bar{p} \tag{19}$$

The expressions for $\bar{\sigma}_1$ and $\bar{\sigma}_3$ can be obtained from the real stress states according to Eq. (7)

$$\bar{\sigma}_1 = \sigma_1 + \left[p_r\left(\frac{p+\sigma_0}{p_r}\right)^n - p\right] \tag{20a}$$

$$\bar{\sigma}_3 = \sigma_3 + \left[p_r\left(\frac{p+\sigma_0}{p_r}\right)^n - p\right] \tag{20b}$$

The value of α can then be determined by solving Eq. (19) in conjunction with Eq. (20).

The other two parameters d and β can be determined from the test results at $\theta = 120°$ and $\theta = 180°$. For example, at $\theta = 120°$, $\bar{\sigma}_1 > \bar{\sigma}_2 = \bar{\sigma}_3$ and $A = 0.5$, we have

$$\bar{\sigma}_1 - \bar{\sigma}_3 = M_f\bar{p}\exp\left[d(2.25 + 1.5\beta)\right] \tag{21}$$

While at $\theta = 180°$, $\bar{\sigma}_1 = \bar{\sigma}_2 > \bar{\sigma}_3$ and $A = 1$, we have

$$\alpha(\bar{\sigma}_1 - \bar{\sigma}_3) + (1-\alpha)(\bar{\sigma}_1 - \bar{\sigma}_3)\frac{2\bar{\sigma}_1 + \bar{\sigma}_3}{\bar{\sigma}_1 + 2\bar{\sigma}_3} = M_f\bar{p}\exp\left[d(4 + 2\beta)\right] \tag{22}$$

Using the α which has already been determined, d and β can be solved from Eqs. (21) and (22) collectively. To capture the overall trend of strength variation, it is sometimes necessary to slightly tune the values for α, d and β when the general prediction using these values does not fit the test results very well.

4.1.3. Example case of the isotropically consolidated San Francisco Bay Mud

As a demonstrative example, the model parameters for isotropically consolidated San Francisco Bay Mud with typical cross-anisotropy (Kirkgard and Lade, 1991, 1993) are determined according to the general procedure outlined above, which is itemized as follows.

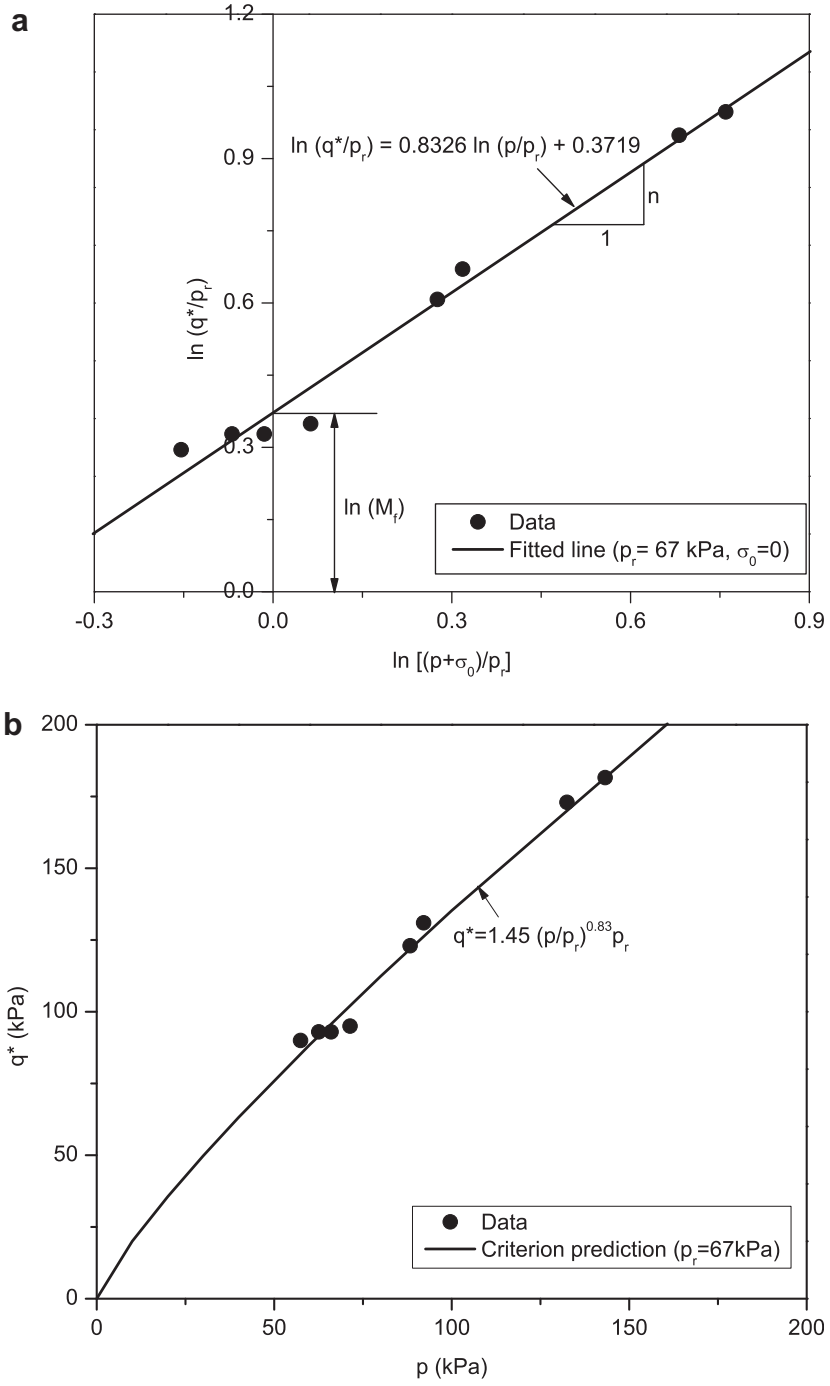

Fig. 10. Determination of M_f and n for isotropically consolidated San Francisco Bay Mud.

(a) σ_0: As discussed before, we assume the triaxial tensile strength $\sigma_0 = 0$.

(b) p_r: The reference pressure is set to be $p_r = 67$ kPa, which is in the vicinity of the mean stress at failure in this series of tests.

(c) M_f and n: In conjunction with Eq. (18) and the test data in the meridian plane as presented by Kirkgard and Lade (1993), a plot in Fig. 10 can be drawn, from which it is readily obtained: $M_f = 1.45$ and $n = 0.83$.

(d) α: The true triaxial test results have been projected on the same deviatoric plane with a mean stress of $p = 167$ kPa and a friction angle of $\varphi_c = 31.6°$ at $\theta = 0°$ by Kirkgard and Lade (1993). These results are employed to determine α first and then d and β. Since the test results exactly at $\theta = 60°$ is not available, we use the stress state of Point A close to $\theta = 60°$ as shown in Fig. 11(a) ($\sigma_1 = 219.3$ kPa and $\sigma_3 = 62.3$ kPa) for this purpose. According to Eqs. (19) and (20) in conjunction with the parameters obtained in Steps a)–c), it is easily to have: $\alpha = 0.49$.

(e) d and β: Noticing that the test data at $\theta = 180°$ (Point D in Fig. 11(a)) is slightly out of the general trend of strength variation, we choose the deviatoric stress at a neighboring Point C (Fig. 11(a)) for the calculation. Using the stress states of Point B at $\theta = 120°$ ($\sigma_1 = 287.6$ kPa and $\sigma_3 = 106.7$ kPa) and Point C ($\sigma_1 = 213.8$ kPa and $\sigma_3 = 73.5$ kPa) in Eqs. (20), (21) and (22), we have $d = 0.013$ and $\beta = -7.69$.

Thus far all the required parameters in the anisotropic failure criterion for isotropically consolidated San Francisco Bay Mud have been calibrated. The model prediction will be compared with the

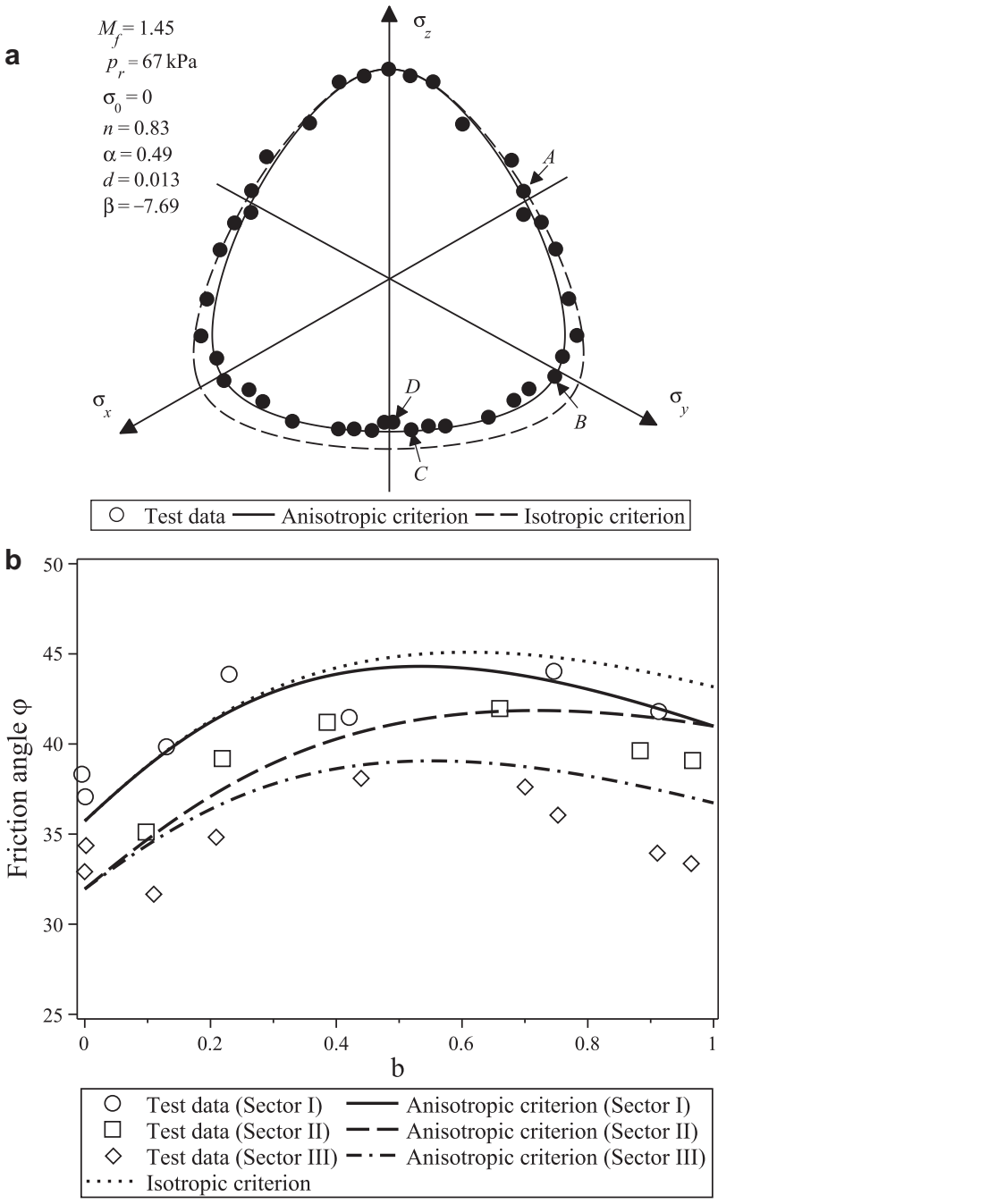

Fig. 11. Comparison of the isotropic and anisotropic failure criteria with experimental data for isotropically consolidated San Francisco Bay Mud (Kirkgard and Lade, 1993), (a) in the deviatoric plane, and (b) in the φ–b diagram.

test data in next section. Essentially the same procedure has been followed to determine the parameters for all the other soils to be discussed in this paper, including the Cambria sand (Ochiai and Lade, 1983), dense Santa Monica beach sand (Abelev and Lade, 2004) as well as Toyoura sand (Lam and Tatsuoka, 1988) in triaxial tests. However, since the available test data in the meridian plane for dense Santa Monica Beach sand and Toyoura sand are not sufficient for determining the curvature of the failure curves, we assume $n = 1$ and calculate M_f based on the friction angle φ_c at $\theta = 0°$ ($M_f = 6\sin\varphi_c/(3 - \sin\varphi_c)$). Note that the values of M_f, p_r, σ_0, n and α for the underlying isotropic failure criterion is assumed to be the same as those for the anisotropic one for each material in the present paper. The parameters determined for these soils are summarized in Table 1.

It will be useful for the readers to have an approximate range for each parameter involved in the failure criterion. Based on our observation on the two clays and four sands from Table 1 as well as our experience gained from the parametric sensitivity study, the following ranges are recommended for clay or sand: (a) $M_f \in [0, 3.0]$; (b) $\sigma_0 = 0$; (c) p_r is in the vicinity of the test pressure; (d) n: close or equal to 1; (e) $\alpha \in [0, 1]$; (f) $d \in [-0.1, 0.1]$ and $d\beta \in [-0.1, 0.1]$. Note that the ranges in item (f) are so provided based on our observation that d and β jointly affect the model prediction.

Table 1
Summary of model parameters calibrated for soils and rocks under study in this paper.

Materials	(Data source)	M_f	p_r	σ_0	n	α	d	β
Clay	Isotropically consolidated San Francisco Bay Mud (Kirkgard and Lade, 1993)	1.45	67 kPa	0	0.83	0.49	0.013	−7.69
	K0-consolidated San Francisco Bay Mud (Lade and Kirkgard, 2000)	1.38	–[a]	0	1	0	0.058	1.44
Sand	Cambria Sand (Ochiai and Lade, 1983)	1.62	–	0	1	0.48	0.014	−3.57
	Dense Santa Monica Beach Sand (Abelev and Lade, 2004)	1.87	–	0	1	0.33	−0.05	−1
	Toyoura Sand (Lam and Tatsuoka, 1988; Tatsuoka et al., 1990)	1.68	–	0	1	0.17	0.05	−2.6
	Dry-pluviated Santa Monica Beach Sand (Lade et al., 2008)	1.63	–	0	1	0.36	−0.04	0
Rock	Touremire Shale (Niandou et al., 1997)	1.58	50 MPa	2.5 MPa	0.54	–	0.5	−1.5
	Angers Schist (Duveau et al., 1998)	2.36	100 MPa	8 MPa	0.76	–	2.5	−1.52

[a] –: not specified.

4.2. For rocks

Rocks are commonly tested under conventional triaxial compression. Using data from triaxial compression tests, we are able to determine such parameters as σ_0, p_r, n and M_f according to the failure curve in the meridian plane, following a similar procedure in Section 4.1.1. In addition, α, d and β need also to be determined. On seeing that Eq. (16) can be simplified as $\bar{q}/\bar{p} = M_f f(A)$ in the triaxial compression mode, α has no effect here and hence needs not to be specified. From Eq. (17), we see that $f(A)$ reaches the minimum when $A = -\beta/2 - 1$, and d is typically positive for rocks according to our experience. As such, β can be back calculated based on the value of A corresponding to the loading direction in which the minimum strength is obtained, and the test results in the $q \sim \xi$ plane can be used for this purpose. The relation between A and ξ can be determined from Eq. (12) by setting $b = 0$. d can then be determined by trial-and-error to best fit the overall test data. Fine tuning to β may be required when the test data are scattered. In this paper, we employ test data on two rocks to verify the anisotropic failure criterion, one for the Touremire shale (Niandou et al., 1997) and the other for a middle Ordovician schist of Angers (France) (Duveau et al., 1998). Model parameters for the two rocks are determined according to the following procedure:

(a) σ_0: The triaxial tensile strength σ_0 of rock is difficult to determine by conventional laboratory tests. As such it is always determined empirically. Here, its value is determined according to Chen et al. (2010) for the Touremire shale as $\sigma_0 = 2.5$ MPa, and according to Mroz and Maciejewski (2002) for the Angers schist as $\sigma_0 = 8$ MPa.
(b) p_r: The reference pressure p_r is chosen at 50 MPa for the Touremire shale and 100 MPa for the Angers schist, respectively. These pressures are within close range of the test pressure of the two rocks.
(c) M_f and n: The parameters M_f and n are determined from the triaxial compression test results with $\theta = 0^\circ$ based on Eq. (18) and a figure similar to Fig. 10(a). Thereby we obtained $M_f = 1.58$ and $n = 0.54$ for the Touremire shale, and $M_f = 2.36$ and $n = 0.76$ for the Angers schist.
(d) α: It needs not to be specified for either rock.
(e) d and β: Note that the minimum strength for both rocks is found near $\xi = 45^\circ$, which corresponds to $A = 0.25$ (Eq. (12)), and hence, $\beta = -2(A + 1) = -1.5$. The value of β will be used for the Touremire shale. Since the results for the Anger schist appear to be quite scattered, the original value of $\beta = -1.5$ has been slightly modified to -1.52 to better fit the overall trend. The value of d is then obtained by curve-fitting the test data set: $d = 0.5$ for the Touremire shale and $d = 2.5$ for the Angers schist.

The obtained model parameters for the two rocks are summarized in Table 1 together with those for the soils. The typical ranges of the parameters for rocks appear to be different from those for soil. Based on limited data, we suggest the following ranges would work reasonably well for most rocks: (a) $M_f \in [0, 3.0]$; (b) σ_0 and p_r: both of them are dependent on the rock type and the test pressure and should be determined with discretion. (c) $n \in [0, 1]$; (e) $\alpha \in [0, 1]$; (f) $d \in [0, 3.0]$; (g) $\beta \approx -1.5$.

5. Comparison with experimental results

5.1. True triaxial tests on soils

5.1.1. Isotropically consolidated San Francisco Bay Mud (Kirkgard and Lade, 1993)

The anisotropic failure criterion proposed in previous sections is first employed to predict the anisotropic strength of isotropically consolidated San Francisco Bay Mud tested by Kirkgard and Lade (1993). The test data are compared in Fig. 11 against the anisotropic failure criteria in Eq. (16) as well as the isotropic failure criterion in Eq. (8) in the deviatoric plane for which $p = 167$ kPa and the plane of $\varphi \sim b$ where φ is the peak friction angle of the soil. The calibrated parameters for the anisotropic criterion are shown in Fig. 11(a).

As is shown in Fig. 11(a), the anisotropic criterion captures the overall trend of the test data in the deviatoric plane reasonably well, only with a slight underestimation of the soil strength in Sector II. In contrast, the isotropic criterion clearly overestimates the strength at large, particularly in Sector III. The tested $\varphi \sim b$ relation and the corresponding predictions of the two failure criteria are also shown in Fig. 11(b). The average mean stress at failure for the experiments on isotropically consolidated San Francisco Bay Mud is about 67 kPa (Lade, 2007) and we use this constant mean stress to perform the prediction for the $\varphi \sim b$ relation in all the three sectors. As is shown in Fig. 11(b), the isotropic criterion gives a single $\varphi \sim b$ relation for all sections which significantly overestimates the value of friction angle in Sectors II and III. The prediction of the anisotropic failure criterion is in good accordance with the test data in Sectors I and II, but slightly overestimates the value of friction angle in Sector III with a maximum difference of 4° at $b = 1$ in sector III, about 10% of the measured friction angle. Nevertheless, we observe an overall satisfactory performance of the anisotropic criterion in predicting the strength anisotropy for isotropically consolidated San Francisco Bay Mud.

5.1.2. Cambria Sand (Ochiai and Lade, 1983)

The anisotropic failure criterion has also been employed to predict the strength of Cambria sand and is compared against the test data obtained by Ochiai and Lade (1983). All the triaxial test results are projected on the same deviatoric plane with a mean stress $p = 334$ kPa (Ochiai and Lade, 1983). The parameters selected for the anisotropic failure criterion for Cambria sand are shown in Fig. 12(a). Presented in the figure is the comparison between model

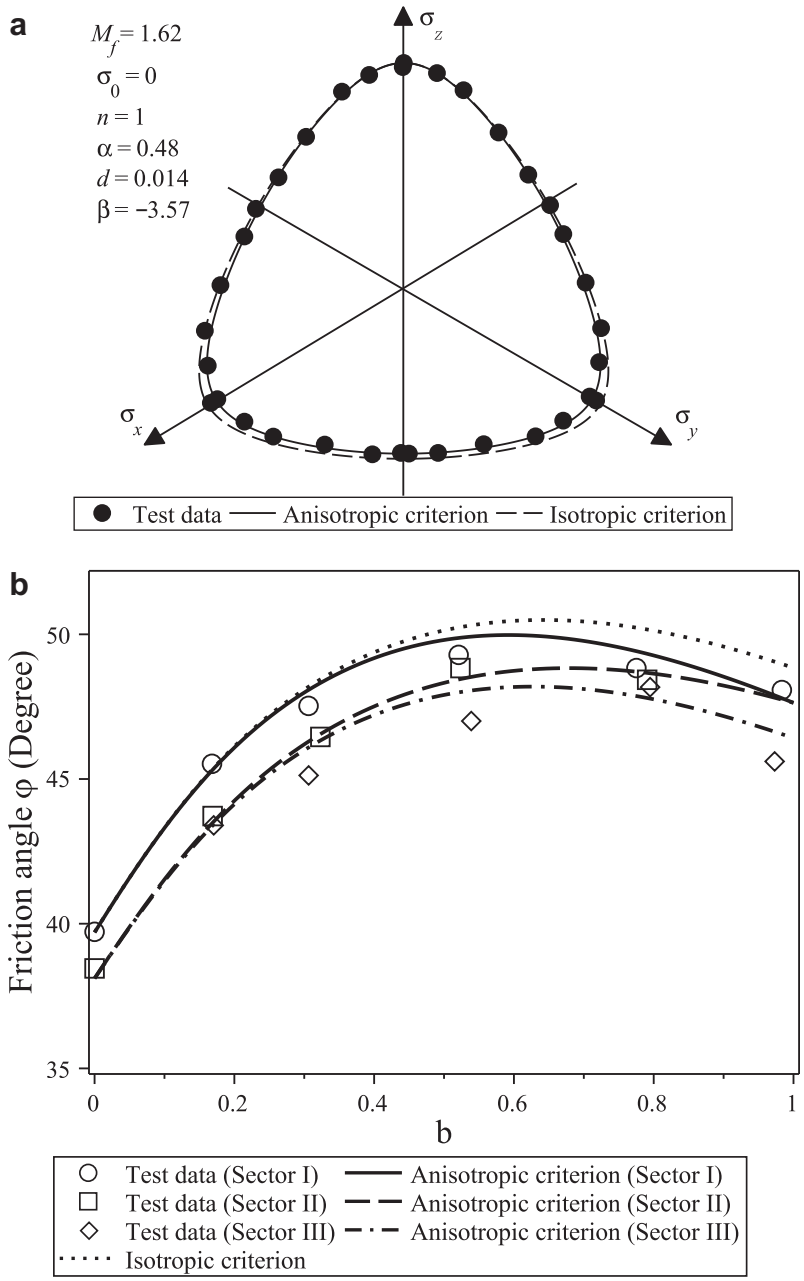

Fig. 12. Comparisons of the test data on Cambria Sand (Ochiai and Lade, 1983) with predictions by the isotropic and anisotropic failure criteria in (a) the deviatoric plane and (b) the $\varphi \sim b$ diagram. Variation of the friction angles shows more significant anisotropic effect than that of the strength in the deviatoric plane does.

prediction by our new anisotropic criterion and the experimental data, along with the prediction by the underlying isotropic criterion in Eq. (8). For Cambria sand, the effect of anisotropy on the failure curve in the deviatoric plane has been found to be relatively small, and the two criteria produce very close predictions (Fig. 12(a)). In the $\varphi \sim b$ plane, however, the variation of friction angle with b demonstrates an obvious dependence on anisotropy in the three sectors, as is shown in Fig. 12(b). The isotropic failure criterion fails to capture this property of the Cambia sand. We also note that the prediction of Lade's anisotropic failure criterion (Lade, 2008) slightly underestimates the φ value at $b = 0.7$ to $b = 1.0$ in all the three sectors. The present anisotropic failure criterion captures the trend of $\varphi \sim b$ relation better in both Sector I and Sector II. It only slightly overestimates the value of φ at $b = 0.3$ to $b = 1.0$ in Sector III by about 1°.

5.1.3. Dense Santa Monica beach sand (Abelev and Lade, 2004)

True triaxial tests have been carried out by Abelev and Lade (2004) on dense Santa Monica beach sand deposited with a cross-anisotropic fabric. All tests have been performed with a constant effective cell pressure of $\sigma_3 = 50$ kPa and a constant value of b. Shear banding was observed in the hardening regime in the midrange of b values in each sector of the deviatoric plane. The parameters selected for the anisotropic failure criterion are shown in Fig. 13(a). As is shown in the figure, the anisotropic failure criterion demonstrates an overall better fitting to the acquired test data than the isotropic failure criterion in both the deviatoric plane and $\varphi \sim b$ diagram. Nevertheless, we also observe in Fig. 13(b) that the peak friction angle of the sand in the midrange of b values for all three sectors is overestimated by the anisotropic failure criterion. The formation of shear banding may be the reason that

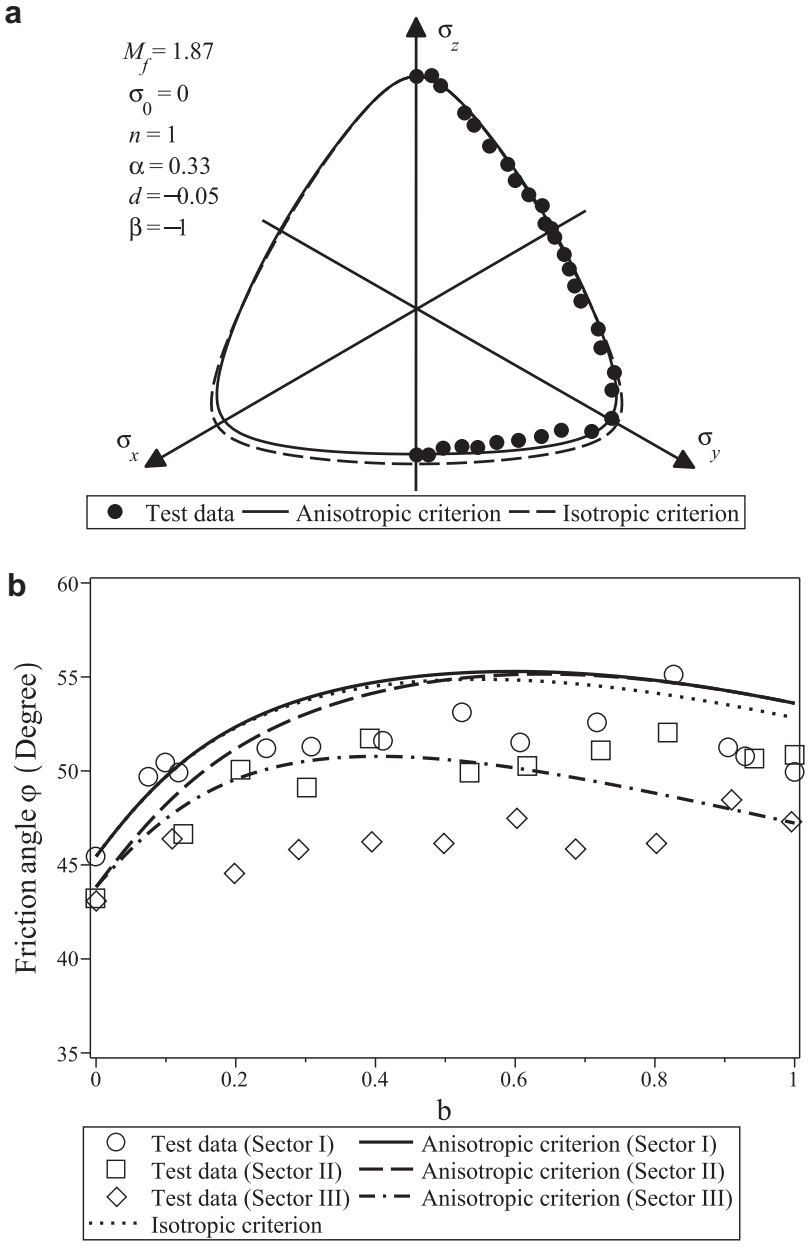

Fig. 13. Failure of dense Santa Monica Beach sand predicted by the isotropic and anisotropic failure criteria in comparison with test data (Abelev and Lade, 2004), in (a) the deviatoric plane and (b) the $\varphi \sim b$ diagram in three sectors. The anisotropic failure criterion overestimates the strength in the midrange of b values due to shear banding.

accounts for this difference in this range of b. Indeed, according to Abelev and Lade (2004) and Lade (2007, 2008), occurrence of shear banding may reduce the strength measured from the boundary of the samples. The anisotropic criterion is therefore expected to serve as a target of strength that the material could have attained if the deformation were uniform in the tested sample. We also comment that the prediction by Lade's anisotropic failure criterion (Lade, 2008) in the deviatoric plane is roughly the same as our prediction using the anisotropic criterion proposed in this paper; whereas for the $\varphi \sim b$ relation, the prediction by Lade (2008) appears to be slightly better.

5.1.4. Toyoura sand (Lam and Tatsuoka, 1988)

Lam and Tatsuoka (1988) carried out true triaxial tests with a constant cell pressure of $\sigma_3 = 98$ kPa on Toyoura sand where the sand samples have been prepared by the air-pluviating method to introduce initial cross-anisotropic fabric. Shear banding has been observed in their testing. The chosen parameters for the anisotropic failure criterion and predicted strength for the sand are presented in Fig. 14, as compared against the experimental data. In the deviatoric plane, the anisotropic failure criterion provides a better correlation with the test data than the isotropic criterion does. It does, however, slightly overestimate the strength in the midrange of b values in Sectors II and III, which is similar to the case of Santa Monica beach sand.

Tatsuoka et al. (1990) have later carried out triaxial compression tests on Toyoura sand. It is also interesting to make a comparison of our model prediction with their experimental data. Presented in Fig. 14(b) is the variation of the friction angle with the loading direction in term of ξ at a constant confining pressure of 98 kPa obtained by the triaxial compression tests (Tatsuoka et al., 1990), in close comparison with the predictions by the

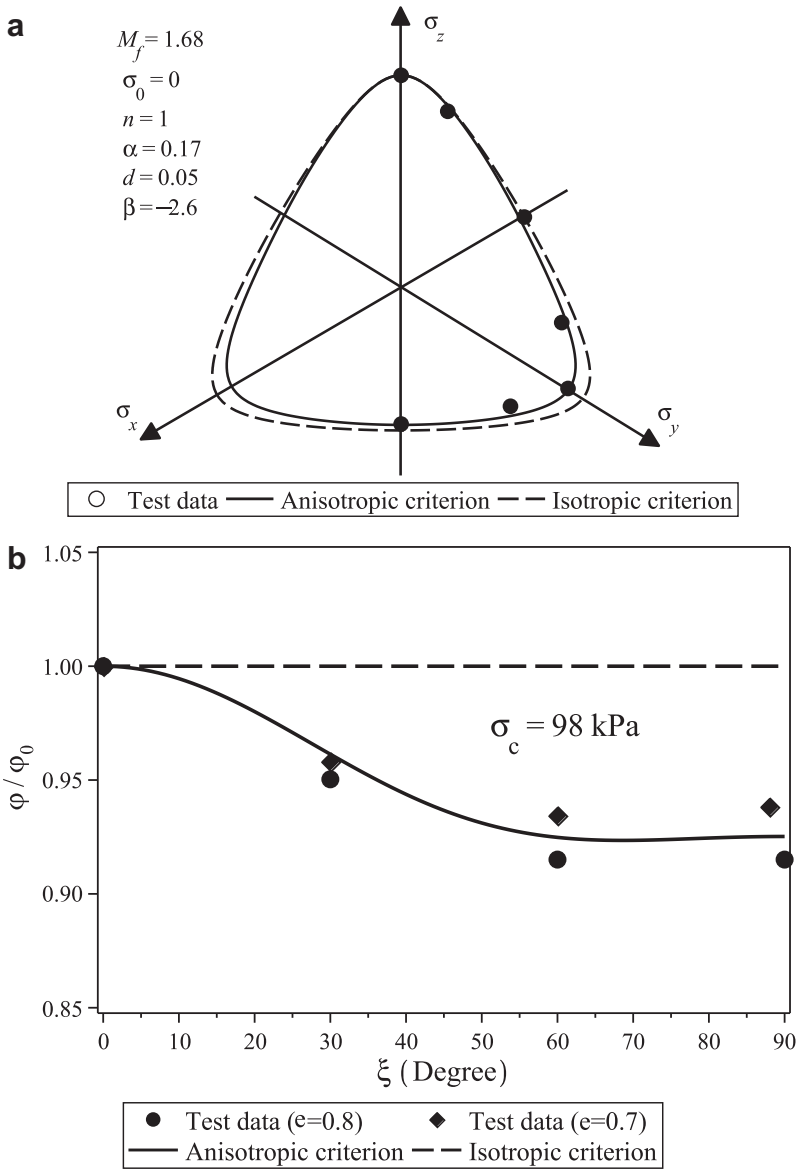

Fig. 14. Prediction of the strength of Toyoura Sand by the isotropic and anisotropic failure criteria in comparison with (a) the true triaxial test results by Lam and Tatsuoka (1988) in the deviatoric plane; and (b) the triaxial compression test results by Tatsuoka et al. (1990) in the $\varphi/\varphi_0 - \xi$ diagram.

isotropic and anisotropic failure criteria. Note that two set of data are presented in the figure which correspond to samples with different initial void ratios. Since the strength of sand is known to be affected by the initial void ratio as well as confining pressure, the data in Fig. 14(b) have been normalized by the friction angle at $\xi = 0°$ (denoted as φ_0) for consistency. No shear banding has been observed in the triaxial compression tests. As is shown in Fig. 14(b), the prediction by the anisotropic failure criterion for the triaxial tests on Toyoura sand compares favorably with the test data, whilst the constant prediction by the isotropic criterion deviates from the test data by a large extent when ξ becomes greater.

5.2. Torsional shear tests

5.2.1. K_0-consolidated San Francisco Bay Mud (Lade and Kirkgard, 2000)

A series of torsional shear tests have been carried out by Lade and Kirkgard (2000) on K_0-consolidated San Francisco Bay Mud using hollow cylinder torsional shear apparatus. Various stress paths were applied to achieve the full range of stress rotation from $\zeta = 0°$ to $\zeta = 90°$. In their tests, the pressures applied to the inside and outside walls of the cylinder were maintained at the same value, such that the following relation between b and ζ holds

$$b = \sin^2 \zeta \tag{23}$$

As there are not sufficient test results available in the meridian plane, we assume here $n = 1$ and $\sigma_0 = 0$ kPa for simplicity. M_f is calculated based on the friction angle ($\varphi_c = 34.1°$) at $b = 0$, which corresponds to the conventional triaxial compression shear mode. d and β are determined based on the results at $b = 0.5$ and $b = 1.0$ by assuming $\alpha = 0$. Presented in Fig. 15 is the comparison between the test data and the prediction of the anisotropic criterion. The anisotropic failure criterion demonstrates a better performance in the prediction than the isotropic one. Nevertheless, it still overestimates the values of friction angle when $0.1 < b < 0.4$. Note that Lade and Kirkgard (2000) have remarked that the K_0-consolidated samples of San Francisco bay mud appear to retain the original in situ fabric which is essentially different from that in the isotropically

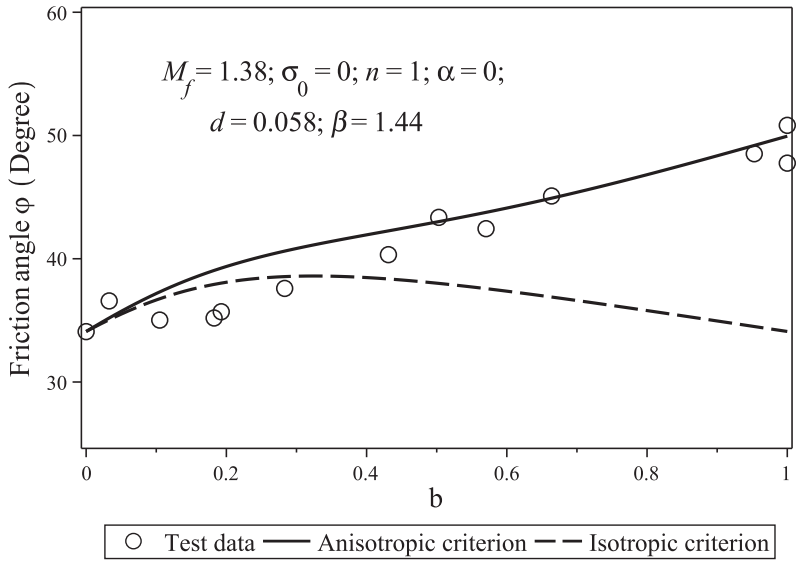

Fig. 15. Comparison between the torsional shear test results on the K_0-consolidated San Francisco Bay Mud (Lade and Kirkgard, 2000) and predictions of the isotropic and anisotropic failure criteria in the $\varphi \sim b$ diagram.

consolidated remolded specimens tested by Kirkgard and Lade (1993).

5.2.2. Santa Monica Beach sand (Lade et al., 2008)

A total of 34 torsional shear tests have been carried out by Lade et al. (2008) on dry-pluviated Santa Monica Beach sand. The tests were conducted under drained conditions at a cell pressure of 200 kPa applied to both the inner and outside cell walls. For comparison with the torsional shear tests, 11 true triaxial tests have also been performed in the cubic triaxial apparatus with four different confining pressures. Since the curvature of the failure curve in the meridian plane can not be determined based on the available test data, n is set to be unity here. M_f is calculated based on the average value of the friction angles obtained in the conventional triaxial compression tests performed in the torsional shear apparatus and the cubic triaxial apparatus respectively ($\varphi_c = 34.1°$). The friction angle obtained in true triaxial tests at $b = 1$ ($\varphi_e = 46°$), which corresponds to the shear modes of $\theta = 60°$ and $\xi = 0°$ as shown in Fig. 3, is used to determine the parameter α in Eq. (19) (see Lade et al. (2008) for data obtained in true triaxial tests). Shear banding has been observed in most of the torsional shear tests by Lade et al. (2008). To minimize the influence of shear banding, we only select the results obtained at $b = 1$, which corresponds to the shear mode of $\theta = 180°$ and $\xi = 0°$as shown in Fig. 3, for determining the parameter d based on Eq. (22) by setting $\beta = 0$. The predictions are presented in Fig. 16, with the parameters chosen for the anisotropic failure criterion shown in Fig. 16(b). Whilst both the isotropic criterion and the anisotropic criterion capture the test data reasonably well in the plane of $(\sigma_z - \sigma_\theta) \sim \sigma_{z\theta}$ in Fig. 16(a), it is in the $\varphi \sim b$ plane that the difference can be depicted. As shown in Fig. 16(b), the isotropic failure criterion clearly overestimates the measured strength when $b > 0.3$. The anisotropic failure criterion, on the other hand, can capture the overall trend of strength variation with b better. Nevertheless, noticeable overestimation is still observed in the range of $0.3 < b < 0.85$ where shear banding comes into effect. The parameters used for soils subjected to torsional shear tests in Figs. 15 and 16 are also listed in Table 1.

5.3. Triaxial compression tests on rocks

Here in this subsection we present a comparison between the predictions of our anisotropic failure criterion with triaxial test data on two rocks reported in the literature, one on the Touremire shale in Niandou et al. (1997) and the other on the Angers schist (Duveau et al., 1998). Both rocks have been found to exhibit strong strength anisotropy. In Figs. 17 and 18 are the comparison results of our anisotropic criterion with experimental data on the two rocks, respectively. Predictions by the isotropic criterion are also shown for the convenience of comparison.

As is shown in Fig. 17 for the Touremire shale, the anisotropic failure criterion satisfactorily captures the $p \sim q$ relation at different loading directions (Fig. 17(a)). Its predictions also agree well with the test data at most confining pressure levels, only with slight overestimation of the strength at a low confining pressure of $\sigma_c = 1$ MPa when $\xi > 0°$ and moderate underestimation for the case of $\sigma_c = 20$ MPa (Fig. 17(b)). The possible reason for the observed deviation may lie in that the anisotropic variable A introduced in this paper is assumed to be only a measure of the stress direction relative to the material fabric orientation but independent on the mean stress. According to Niandou et al. (1997), the degree of strength anisotropy is greater at lower confining pressure levels than that at higher one. This pressure-dependent strength anisotropy has also been observed by Lade and Abelev (2005) in sand. A potential improvement of the current anisotropic failure criterion may be to incorporate the effect of mean stress, e.g., in the anisotropic variable A.

The test data for the Angers schist are more scattered compared to those for the Touremire shale (Fig. 18). Our anisotropic failure criterion, with the chosen parameters shown in Fig. 18(b), can reasonably capture the overall trend of the data set in both the $p \sim q$ and $\xi \sim q$ planes. In the $\xi \sim q$ plane as shown in Fig. 18(b), the criterion is found to predict a slightly higher strength at all range of ξ except $\xi = 0°$ and 90°. The isotropic failure criterion fails to capture the strength variation with loading directions for both rocks in either the $p \sim q$ plane or the $\xi \sim q$ plane.

6. Conclusion

A general anisotropic failure criterion has been proposed to describe the failure of geomaterials. An anisotropic variable A in terms of the invariants and joint invariants of the stress tensor and the fabric tensor is introduced into the new anisotropic criterion to characterize the loading direction with respect to the fabric orientation. The frictional parameter M_f in an isotropic criterion

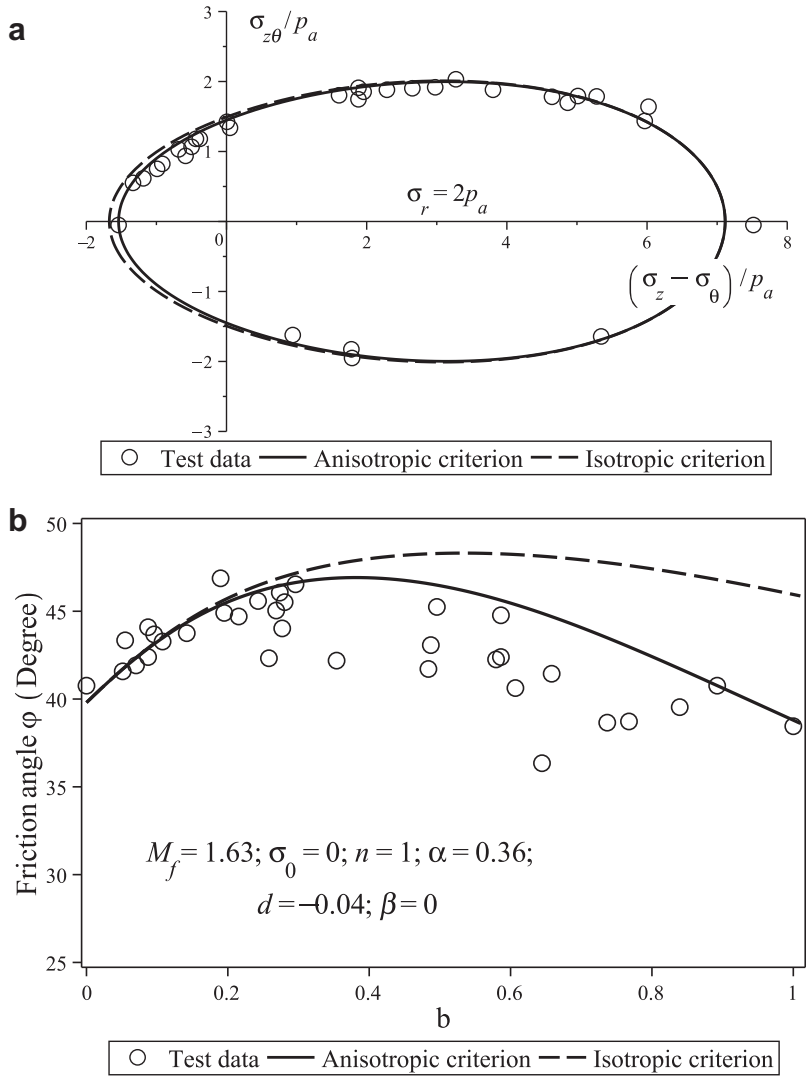

Fig. 16. Comparison between the torsional shear test results on dry-pluviated Santa Monica Beach sand (Lade et al., 2008) with the predictions by the isotropic/anisotropic failure criteria in (a) the $\sigma_{z\theta} \sim (\sigma_z - \sigma_\theta)$ diagram, and (b) the $\varphi \sim b$ diagram.

proposed by Yao et al. (2004) is then modified to accommodate this newly defined A and two other parameters which combine to account for the overall influence of loading direction and the degree of cross-anisotropy on the strength of soil or rock. The anisotropic criterion has been presented in general forms in both the deviatoric plane and the meridian plane, which lends it the generality to describe the failure of a material under general loading conditions. By choosing the conventional triaxial compression shear mode as a reference state (the anisotropic failure criterion is identical to the isotropic one at this state) supplemented with other available information, it is convenient to calibrate the parameters introduced in the new criterion.

The proposed anisotropic failure criterion has been applied to the prediction of failure for a number of different clays, sands as well as rocks, including isotropically consolidated San Francisco Bay Mud in true triaxial tests (Kirkgard and Lade, 1993), K_0consolidated San Francisco Bay Mud in torsional shear tests (Lade and Kirkgard, 2000), Cambria Sand in true triaxial tests (Ochiai and Lade, 1983), Santa Monica Beach sand in true triaxial tests (Abelev and Lade, 2004) and torsional shear tests (Lade et al., 2008), Toyoura sand in true triaxial tests (Lam and Tatsuoka, 1988) and triaxial compression tests (Tatsuoka et al., 1990), as well as two rocks in triaxial compression tests (Niandou et al., 1997; Duveau et al., 1998). The predictions by our anisotropic criterion are in good accordance with the experimental data of these soils and rocks. Discussion is made on the present criterion in comparison with some of the existing ones in the literature.

Shear banding has been observed in the hardening regime in true triaxial tests on sand (Wang and Lade, 2001; Abelev and Lade, 2003) in the midrange of b values (from about 0.18 to approximately 0.85) in the three sectors as shown in Fig. 3. The occurrence of shear banding in the hardening regime prevents the attainment of a smooth peak on the stress–strain relation for which a failure criterion tends to fit with. It has also been observed that, for the range of b that shear banding occurs, the current anisotropic failure criterion slightly overestimates the strength of the soils in the deviatoric plane. The same behavior has been validated by our model prediction here as well. In this case, the prediction of strength by our criterion can be regarded as a targeted upper bound that a soil can achieve if the deformation is uniform in the tested sample. It is noteworthy that the anisotropic variable A used in this paper is only a measure of the relative orientation between the stress and fabric tensors and is independent on the value of mean stresses, which renders the current failure criterion unable to well describe the pressure-dependent strength anisotropy of rocks.

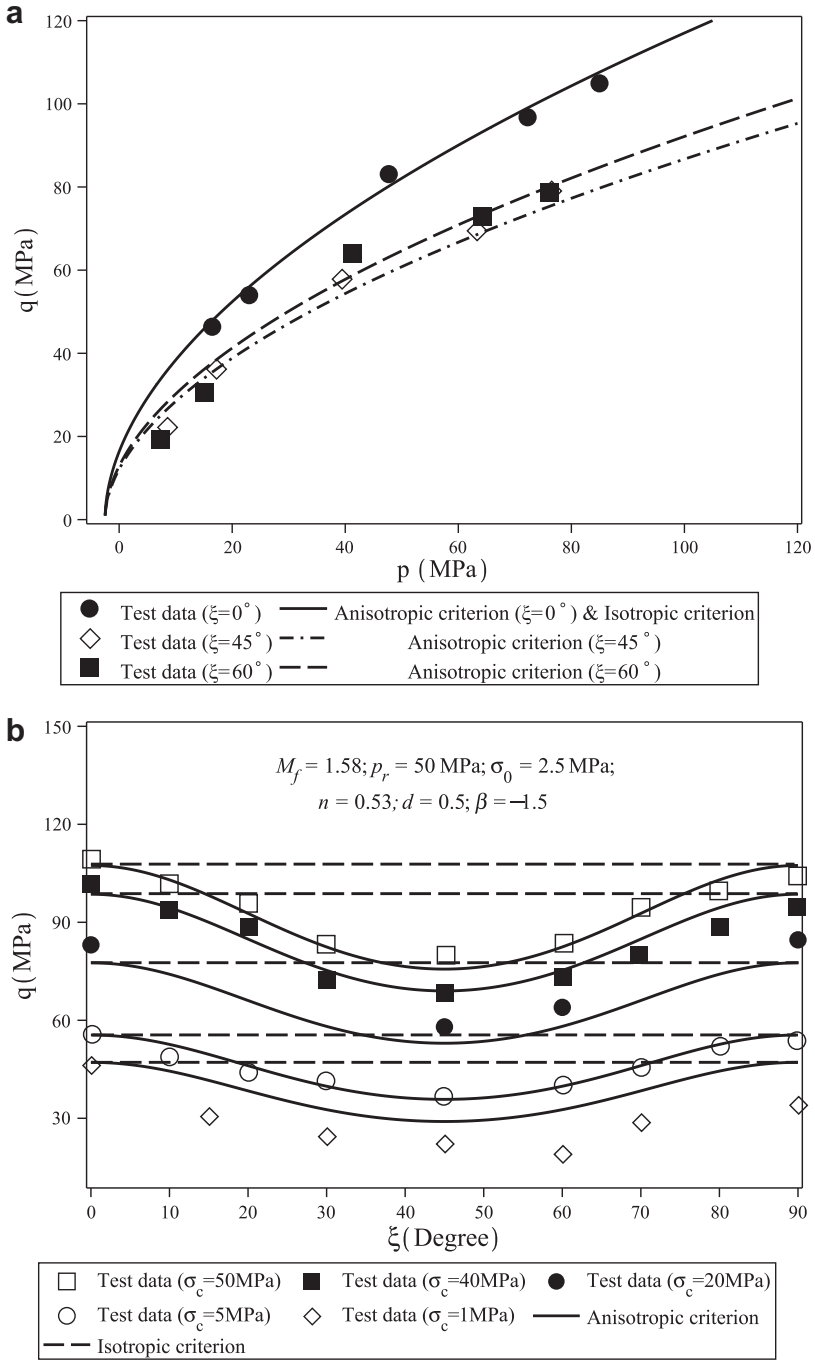

Fig. 17. Comparison between the triaxial compression test data on the Touremire shale (Niandou et al., 1997) and the prediction of the anisotropic and underlying isotropic failure criteria in (a) the $p \sim q$ diagram with different loading directions and (b) the $\xi \sim q$ diagram with different confining pressures.

Further improvement can be made by including an appropriate expression of A with the mean stress as a variable into the criterion.

The anisotropic failure criterion presented in this paper can be conveniently used for constitutive modeling as well. The new criterion can be incorporated into an existing model, such as the Cam-Clay models, to modify their description of both yielding and failure. If hardening needs to be considered, one can simply assume M_f to be a function of the hardening parameter (s) and use the new failure criterion as the yield function (see, e.g., Pietruszczak et al., 2002; Azami et al., 2009). In order to simulate the behavior at constant stress ratio path, it is also possible to introduce a cap in the meridian plane based on the proposed failure criterion, similar to the way adopted by Mortara (2009) and Schweiger et al. (2009).

Note also that the anisotropic failure criterion proposed in this paper has been compared against experimental data on clays, sands and rocks. Its usefulness, however, is not limited to these materials only. For any materials that exhibit appreciable strength anisotropy, such as concrete, ceramics, porous metals, polymers and solid metals as treated by Lade (1997), the failure criterion can be equally useful. The specific procedures in determining the required parameters may differ from those mentioned in this

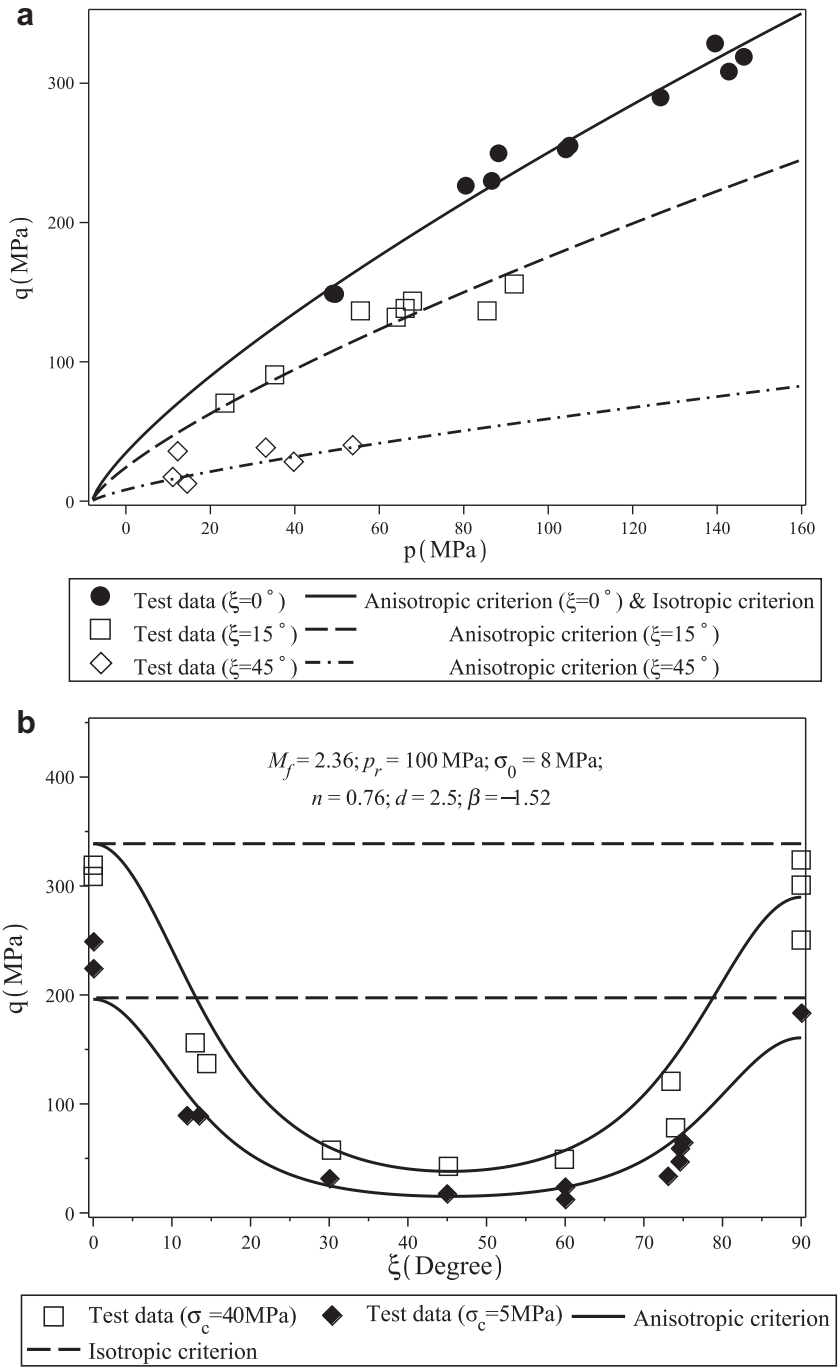

Fig. 18. Comparisons of the triaxial compression test data on the Angers schist (Duveau et al., 1998) with the prediction of the anisotropic and underlying isotropic failure criteria in (a) the $p \sim q$ diagram with different loading directions and (b) the $\xi \sim q$ diagram with different confining pressures.

paper, depending on the availability of routine tests on these different materials.

Acknowledgements

This work was supported by Research Grants Council of Hong Kong (under Grant No. 623609, 622910 and DAG08/09.EG04).

References

Abelev, A.V., Lade, P.V., 2003. Effects of cross-anisotropy on three-dimensional behavior of sand. I: stress-strain behavior and shear banding. J. Eng. Mech. ASCE 129 (2), 160–166.

Abelev, A., Lade, P.V., 2004. Characterization of failure in cross-anisotropic soils. J. Eng. Mech. ASCE 130 (5), 599–606.

Argyris, J.H., Faust, G., Szimmat, J., Warnke, E.P., Willam, K.J., 1974. Recent developments in the finite element analysis of prestressed concrete reactor vessels. Nucl. Eng. Des. 28 (1), 42–75.

Arthur, J.R.F., Menzies, B.K., 1972. Inherent anisotropy in a sand. Géotechnique 22 (1), 115–128.

Attewell, P.B., Sandford, M.R., 1974. Intrinsic shear strength of a brittle, anisotropic rock-I: experimental and mechanical interpretation. Int. J. Rock Mech. Min. Sci. & Geomech. Abstr. 11 (1), 423–430.

Azami, A., Pietruszczak, S., Guo, P., 2009. Bearing capacity of shallow foundations in transversely isotropic granular media. Int. J. Numer. Anal. Meth. Geomech. doi:10.1002/nag.827.

Bishop, A.W., 1971. Shear strength parameters for undisturbed and remoulded soil specimens. Roscoe Memorial Symposium. pp.3–58.

Brewer, R., 1964. Fabric and Mineral Analysis of Soils. Wiley, New York.

Casagrande, A., Carillo, N., 1944. Shear failure of anisotropic materials. J. Boston Soc. Civ. Eng. 31 (4), 74–87.
Chen, L., Shao, J.F., Huang, H.W., 2010. Coupled elastoplastic damage modeling of anisotropic rocks. Comput. Geotech. 37, 187–194.
Dafalias, Y.F., Papadimitriou, A.G., Li, X.S., 2004. Sand plasticity model accounting for inherent fabric anisotropy. J. Eng. Mech. ASCE 130 (11), 1319–1333.
Drucker, D.C., Prager, W., 1952. Soil mechanics and plastic analysis or limit design. Quart. Appl. Math. 10 (2), 157–165.
Duncan, J.M., Seed, H.B., 1966. Strength variation along failure surfaces in clay. J. Geotech. Eng. Div. ASCE 92 (SM6), 81–104.
Duveau, G., Shao, J.F., Henry, J.P., 1998. Assesment of some failure criteria for strongly anisotropic geomaterials. Mech. Cohes-Frict. Mater. 3, 1–26.
Guo, P., 2008. Modified direct shear test for anisotropic strength of sand. J. Geotech. and Geoenvir. Eng. ASCE 134 (9), 1311–1318.
Guo, P., Stolle, D.F.E., 2005. On the failure of granular materials with fabric effects. Soils Found. 45 (4), 1–12.
Habib, P., 1953. Influence de la variation de la contrainte principale moyenne sur la résistance au cisaillement des sols. Proc. Third ICSMFE 1, 131–136.
Hight, D.W., Gens, A., Symes, M.J., 1983. The development of a new hollow cylinder appratus for investigating the effects of principal stress rotation in soils. Géotechnique 33 (4), 355–383.
Houlsby, G.T., 1986. A general failure criterion for frictional and cohesive materials. Soils Found. 26 (2), 97–101.
Imam, S.M.R., Chan, D.H., Robertson, P.K., Morgenstern, N.R., 2002. Anisotropic yielding of loose sand. Soils Found. 42 (3), 33–44.
Kim, M.K., Lade, P.V., 1984. Modeling rock strength in three dimensions. Int. J. Rock Mech. Min. Sci. Geomech. Abstr. 21 (1), 21–33.
Kirkgard, M.M., Lade, P.V., 1991. Anisotropy of normally consolidated San Francisco Bay Mud. Geotech. Test. J., ASTM 14 (3), 231–246.
Kirkgard, M.M., Lade, P.V., 1993. Anisotropic three-dimensional behavior of a normally consolidated Clay. Can. Geotech. J. 30 (4), 848–858.
Lade, P.V., 1977. Elasto-plastic stress–strain theory for cohesionless soil with curved yield surfaces. Int. J. Solids Struct. 13 (11), 1019–1035.
Lade, P.V., 1997. Modelling the strengths of engineering materials in three dimensions. Mech. Cohes-Frict. Mater. 2, 339–356.
Lade, P.V., 2007. Modeling failure in cross-anisotropic frictional materials. Int. J. Solids Struct. 44 (16), 5146–5162.
Lade, P.V., 2008. Failure criterion for cross-anisotropic soils. J. Geotech. and Geoenvir. Eng. ASCE 134 (1), 117–124.
Lade, P.V., Abelev, A., 2005. Characterization of cross-anisotropic soil deposits from isotropic compression tests. Soils Found. 45 (5), 89–102.
Lade, P.V., Duncan, J.M., 1975. Elastoplastic stress-Strain theory for cohesionless soil. J. Geotech. Eng. Div. ASCE 101 (GT10), 1037–1053.
Lade, P.V., Kirkgard, M.M., 2000. Effects of stress rotation and changes of *b*-values on cross-anisotropic behavior of natural K_0-consolidated soft clay. Soils Found. 40 (6), 93–105.
Lade, P.V., Nam, J., Hong, W.P., 2008. Shear banding and cross-anisotropic behavior observed in laboratory sand tests with stress rotation. Can. Geotech. J. 45, 74–84.
Lam, W.K., Tatsuoka, F., 1988. Effects of initial anisotropic fabric and σ_2 on strength and deformation characteristics of sand. Soils Found. 28 (1), 89–106.
Lee, Y.K., Pietruszczak, Z., 2008. Application of critical plane approach to the prediction of strength anisotropy in transversely isotropic rock masses. Int. J. Rock Mech. Min. Sci. 45 (4), 513–523.
Li, X.S., Dafalias, Y.F., 2002. Constitutive modeling of inherently anisotropic sand behavior. J. Geotech. Geoenvir. Eng. ASCE 128 (10), 868–880.
Liu, M.D., Carter, J.P., 2003. General strength criterion for geomaterials. Int. J. Geomech. ASCE 3 (2), 253–259.
Matsuoka, H., Nakai, T., 1974. Stress-deformation and strength characteristics of soil under different principal stresses. Proc., JSCE 232, 59–70.
Mitchell, J.K., Soga, K., 2005. Fundamentals of soil behavior, third ed. John Wiley & Sons, Inc..
Miura, S., Toki, S., 1984. Anisotropy in mechanical properties and its simulation of sands sampled from natural deposits. Soils Found. 24 (3), 69–84.
Mortara, G., 2008. A new yield and failure criterion for geomaterials. Géotechnique 58 (2), 125–132.
Mortara, G., 2009. A yield criterion for isotropic and cross-anisotropic cohesive-frictional materials. Int. J. Numer. Anal. Meth. Geomech. doi:10.1002/nag.846.
Mroz, Z., Maciejewski, J., 2002. Failure criteria of anisotropically damaged materials based on the critical plane concept. Int. J. Numer. Anal. Meth. Geomech. 26, 407–431.
Muhunthan, B., Chameau, J.L., 1997. Void fabric tensor and ultimate state surface of soils. J. Geotech. Geoenvir. Eng. ASCE 123 (2), 173–181.
Niandou, H., Shao, J.F., Henry, J.P., Fourmaintraux, D., 1997. Laboratory investigation of the behaviour of Tournemire shale. Int. J. Rock Mech. Min. Sci. 34 (1), 3–16.
Nishimura, S., Minh, N.A., Jardine, R.J., 2007. Shear strength anisotropy of natural London clay. Géotechnique 57 (1), 49–62.
Ochiai, H., Lade, P.V., 1983. Three-dimensional behavior of sand with anisotropic fabric. J. Geotech. Eng. 109 (10), 1313–1328.
Oda, M., 1972. Initial fabrics and their relations to mechanical properties of granular materials. Soils Found. 12 (1), 17–36.
Oda, M., 1984. Similarity rule of crack geometry in statistically homogeneous rock masses. Mech. Mater. 3 (2), 119–129.
Oda, M., Koishikawa, I., Higuchi, T., 1978. Experimental study of anisotropic shear strength of sand by plane strain test. Soils Found. 18 (1), 25–38.
Oda, M., Nakayama, H., 1989. Yield function for soil with anisotropic fabric. J. Eng. Mech. ASCE 115 (1), 89–104.
Ottosen, N.S., 1977. A failure criterion for concrete. J. Geotech. Eng. Div. ASCE 103 (4), 527–535.
Pietruszczak, S., Lydzba, D., Shao, J.F., 2002. Modelling of inherent anisotropy in sedimentary rocks. Int. J. Solids Struct. 39, 637–648.
Pietruszczak, S., Mroz, Z., 2000. Formulation of anisotropic failure criteria incorporating a microstructure tensor. Comput. Geotech. 26 (2), 105–112.
Pietruszczak, S., Mroz, Z., 2001. On failure criteria for anisotropic cohesive-frictional materials. Int. J. Numer. Anal. Meth. Geomech. 25 (5), 509–524.
Pradhan, T.B.S., Tatsuoka, F., Horii, N., 1988. Simple shear testing on sand in a torsional shear apparatus. Soils Found. 28 (2), 95–112.
Schweiger, H.F., Wiltafsky, C., Scharinger, F., Galavi, V., 2009. A multilaminate framework for modelling induced and inherent anisotropy of soils. Géotechnique 59 (2), 87–101.
Tatsuoka, F., Nakamura, S., Huang, C.C., Tani, K., 1990. Strength anisotropy and shear band direction in plane strain tests of sand. Soils Found. 30 (1), 35–54.
Tatsuoka, F., Sakamoto, M., Kawamura, T., Fukushima, S., 1986a. Strength and deformation characteristics of sand in plane strain compression at extremely low pressures. Soils Found. 26 (1), 65–84.
Tatsuoka, F., Sonoda, S., Hara, K., Fukushima, S., Pradhan, T.B.S., 1986b. Failure and deformation of sand in torsional shear. Soils Found. 26 (4), 79–97.
van Eekelen, H.A.M., 1980. Isotropic yield surface in three dimensions for use in soil mechanics. Int. J. Numer. Anal. Meth. Geomech. 4 (1), 89–101.
Wang, C.C., 1970. A new representation theorem for isotropic functions: an answer to Professor G.F. Smith's criticism of my papers on representations for isotropic functions. Arch. Rational Mech. Anal. 36 (3), 166–197.
Wang, Q., Lade, P.V., 2001. Shear banding in true triaxial tests and its effect on failure in sand. J. Eng. Mech. ASCE 127 (8), 754–761.
Yamada, Y., Ishihara, K., 1979. Anisotropic deformation characteristics of sand under three-dimensional stress conditions. Soils Found. 19 (2), 79–94.
Yang, Z.X., Li, X.S., Yang, J., 2008. Quantifying and modelling fabric anisotropy of granular soils. Géotechnique 58 (4), 237–248.
Yao, Y.P., Lu, D.C., Zhou, A.N., Zou, B., 2004. Generalized non-linear strength theory and transformed stress space. Sci. China E: Tech. Sci. 47 (6), 691–709.
Yoshimine, M., Ishihara, K., Vargas, W., 1998. Effects of principal stress direction and intermediate principal stress on undrained shear behavior of sand. Soils Found. 38 (3), 179–188.
Yong, R.N., Silvestri, V., 1979. Anisotropic behaviour of a sensitive clay. Can. Geotech. J. 16, 335–350.